Universitetet
i Stavanger

FACULTY OF SCIENCE AND TECHNOLOGY

MASTER'S THESIS

Study program/specialization: Petroleum Engineering, Drilling	Spring semester, 2007 Open
Author: Dan Ole Vikeså	…… (signature author)
Instructor: Bernt S. Aadnøy, UIS Supervisor(s): Bernt S. Aadnøy, UIS	
Title of Master's Thesis: Borehole stability on Yme Norwegian title: Borehull stabilitet på Yme	
ECTS: 30	
Subject headings: The Inversion Technique In-situ stresses Fracturing Collapse	Pages: 58 + attachments/other: 27 Stavanger, 13. June 2007 Date/year

Preface

This thesis is the final part of my master degree at the University of Stavanger. The thesis is written at the university with guidance from Bernt S. Aadnøy. Data and information about the Yme field are provided by Talisman.

There are some people I would like to thank for helping me completing this thesis.
First of all a thank to Talisman, and in particular Marianne Torstensen and Lukasz Wrobel, for giving me all the data I needed to do this thesis.

A special thanks to Professor Bernt S. Aadnøy, for all the help throughout this project

Stavanger, June 2007

_____

Dan Ole Vikeså

Abstract

The main object of this thesis it to perform an in-situ stress and borehole stability evaluation of the wells in the Yme field.

The Inversion technique was used find the maximum and minimum horizontal stresses. The stresses were found for the whole well and for the location around each casing shoe.
The field was found to be anisotropic.

The outcome of the analysis was used together with data form each well to calculate fracture and collapse gradients for the wells.

The fracturing gradient became unrealistic large for several of the wells, and too low for well 9/2 A-8. The cause for this may be data inconsistency from collection of the data from many different sources. Also a geological uncertainty related to the faults and tectonic forces present represents a factor.

The effect of azimuth and inclination on the stability is commented by comparing the fracture and collapse gradients for the different wells. Azimuth is observed to have a large effect on the fracturing gradient and a smaller effect on the collapse gradient.

Table of contents

1 Introduction

Borehole stability can cause problems in any drilling operations. Stability problems can result in lost time and sometimes also loss of equipment which means extra cost.

Stability problems can appear in both vertical and horizontal well. Long-reach deviate wells are specially known for having problems with the stability.

Stability evaluation of a well represents a classical rock mechanics problem: prediction of a rock's response to mechanical loading.

The main object of this thesis it to perform an in-situ stress and borehole stability evaluation of the wells in the Yme field.
In chapter 2 the geology of the Yme field is presented and also what the predicted recovery and remaining reserves are.
In chapter 3 the stress state is defined, while in chapter 4 stresses in a borehole is presented.
Two failure criterions: Von Mises shear strength and Mohr-Coulomb shear model are presented in chapter 5.
Chapter 6 and 7 shows the theory about the different fracturing data and the methods for normalizing the fracturing data.
In chapter 9 the Inversion Technique is presented, which will be used to find the maximum and minimum horizontal stresses.
Theory about borehole stability is presented in chapter 10, and the different equations for borehole fracturing and collapse are derived.
Modelling of the in-situ stress field is shown in chapter 11, and the fracture and collapse calculations are done in chapter 12.

Most of the theory is taken from Bernt S. Aadnøy[3]'s "An introduction to petroleum rock mechanics". Also Ann Kristin Hansen[5]'s master thesis "Analysis of Borehole stability on Snorre TLP", has been used as help in this thesis.

2 Geology

The current licence was awarded in 2004, with current licensees being Talisman (70%), Revus Energy ASA (20%) and Petra ASA (10%). The licensees have determined after several reanalysis of the Yme reservoir, that redevelopment of Yme is technically feasible and economically viable.

2.1 Geography[1]

The Yme field lies approximately 100km from the Norwegian coastline in the Egersund basin. It consists of two main tectonic structures named Gamma and Beta. Major faults subdivide each of the structures into distinct reservoirs. Beta consists of three separate segments: East, North-West and South-West. Gamma consists of two segments: West and South-East, and with an un-drilled prospect called Gamma North-East.
Statoil produced from 1996 to 2001 from both Beta and Gamma structures.

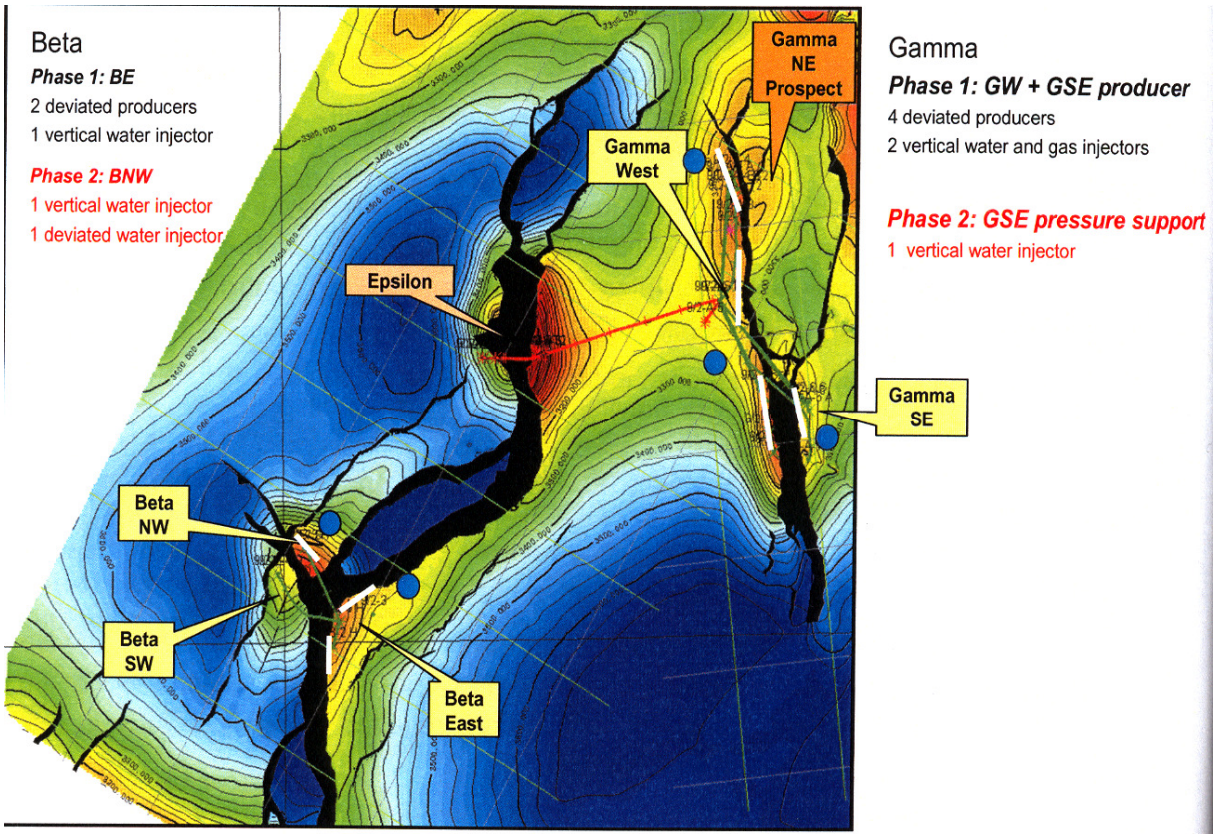

Figure 2.1: Yme Field overview[1]

2.2 Regional geology[1]

There are two main fault trends observed n the Egersund basin adjacent to the Yme field: Fault trend defined by the Tornquist fault zone (NW-SE) and (2) faults of Permian age trending north to south. The basin is bounded to the north-east by the Precambrian Stavanger Platform. The north-western and south-eastern boundaries are defined by the Sele High and Lista Fault Complex, whereas the south-west is bounded by the Åsta Graben/Norwegian-Danish basin.

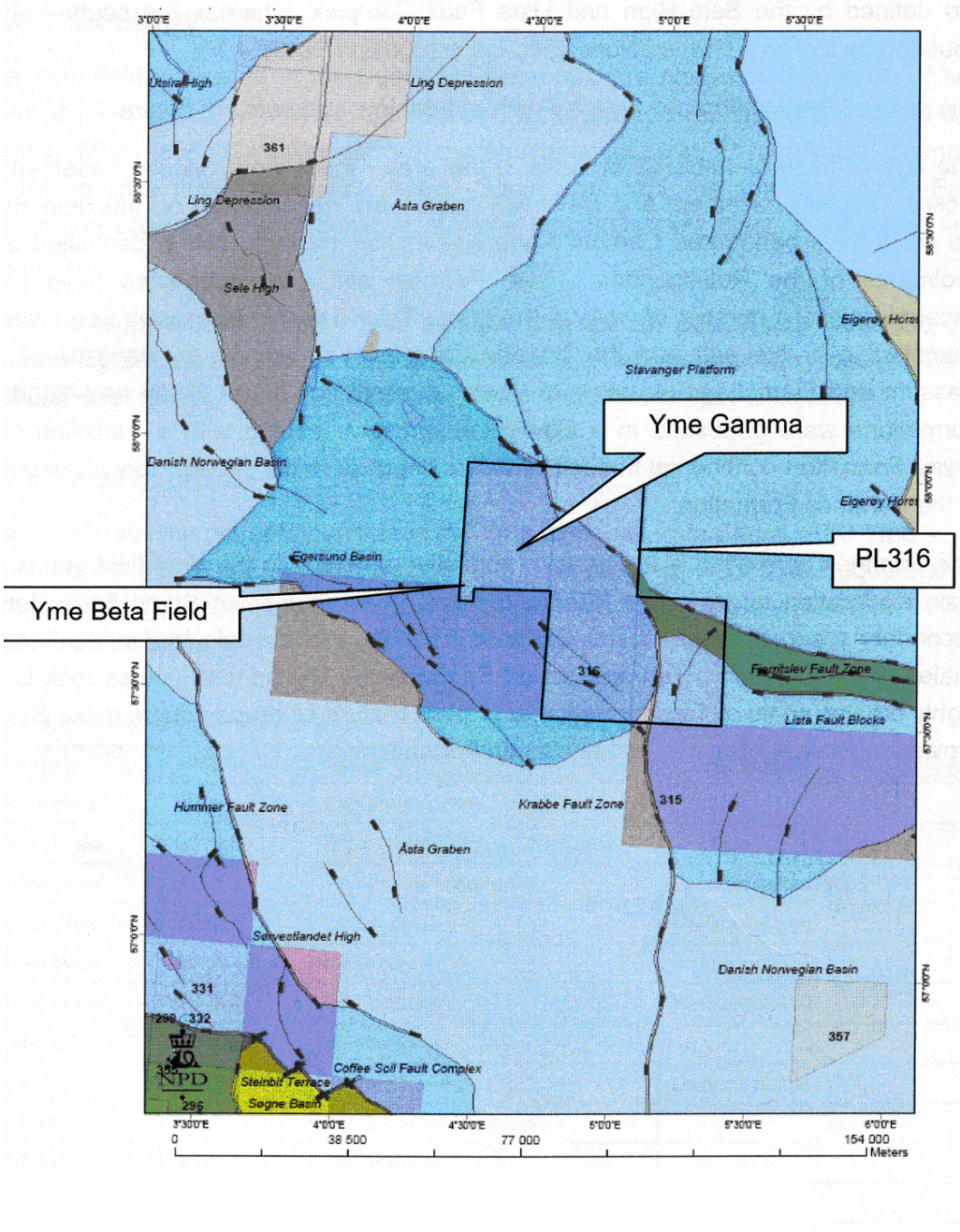

Figure 2.2: Structural framework of Egersund basin[1]

The general lithostratigraphy for the Egersund basin is illustrated in Figure 2.3

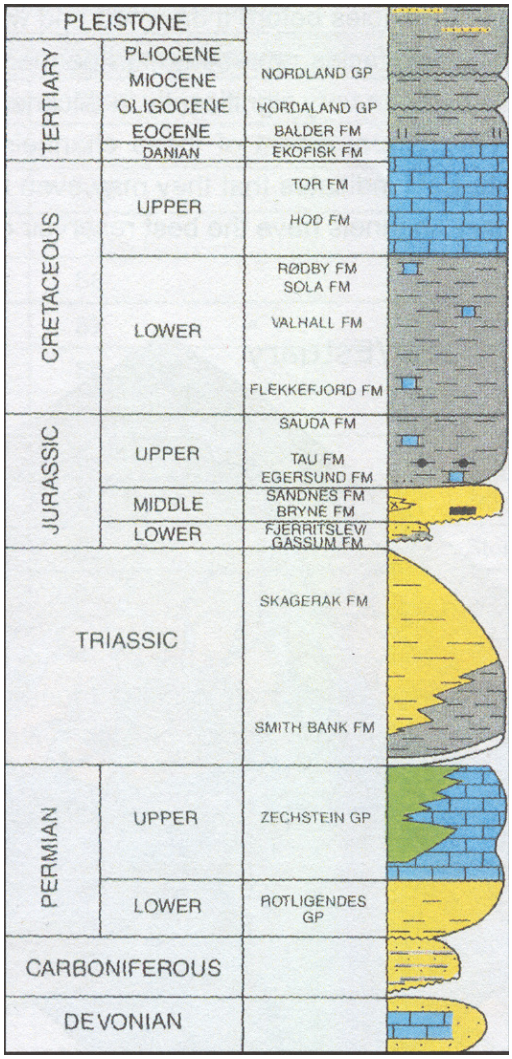

Figure 2.3: General lithostratigraphy for the Egersund basin[1]

The age of the rocks penetrated by the wells in the area ranges from Silurian basement to recent. Silurian basement and Devonian rocks were encountered on the Sele High. The Bryne and Sandnes formations were deposited in a slowly transgressive setting with a transition from Bryne formation continental floodplain/deltaic deposits to the shallow marine deposits of the Sandnes formation.

The Sandnes Formation is the proven productive reservoir in the Yme field and is the main exploration target in the Egersund basin. The underlying Bryne formation is the secondary reservoir target. The Sandnes formation is overlain by Upper Jurassic shales of the Egersund, Tau and Sauda formation. The primary source rock is the highly organic shale of Tau formation. Seal is provided by the Egersund, Tau and Sauda formation.

2.3 Tectonic model[1]

2.3.1 Yme Gamma

The structural framework of the Yme Gamma is essentially split into 2 segments; Gamma West (GW) and Gamma South-East (GSE) (Figure 2.4). Gamma West is a single continuous accumulation. It is a three-way dip closure (west, south and north) with an up-thrown fault closure to the east. The entire structure is formed by tectonics related to a Zechstein salt ridge which has a greater impact in the southern part of the Gamma area (Figure 2.5).
Gamma South-East is the hanging-wall to the southern part of Gamma West and is fault seal dependent towards the west and structurally closed towards the east.

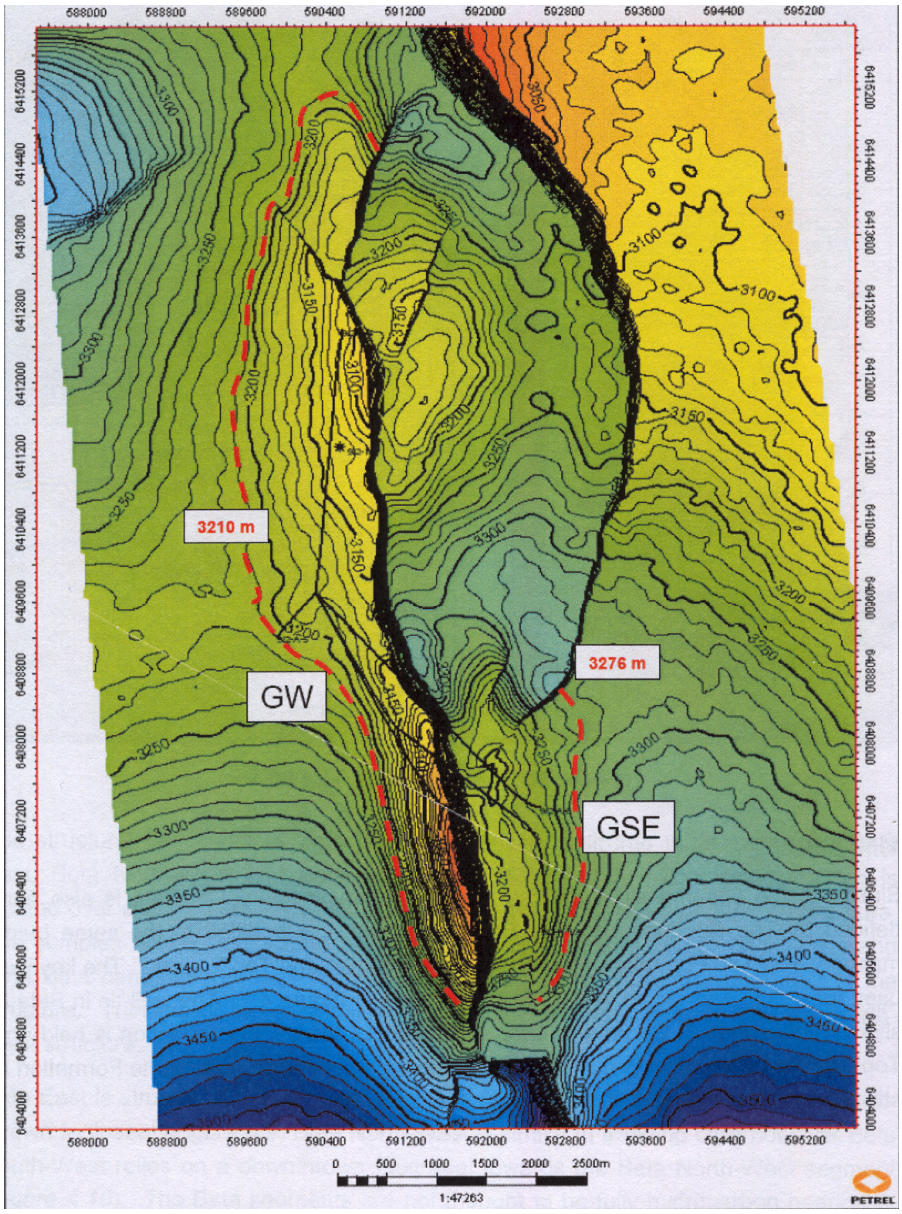

Figure 2.4: Top Sandnes Formation structural depth map[1]

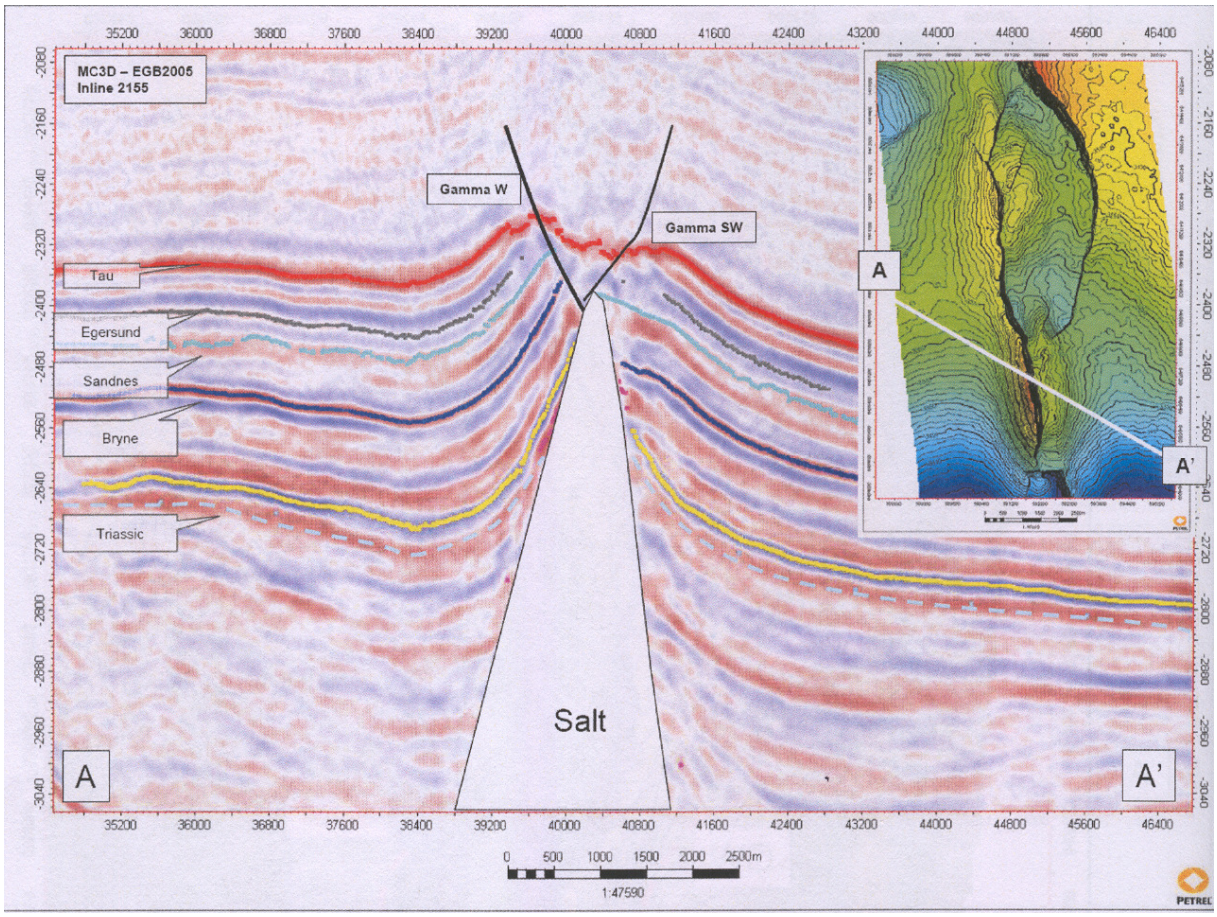

Figure 2.5: Yme Gamma SW and SE[1]

2.3.2 Yme Beta

The structural framework of the Yme Beta is essentially spilt into 3 segments; Beta East (BE), Beta North-West (BNW) and Beta South-West (BSW) (Figure 2.6). The Beta structure is located over a large Zechstein salt pillow, which influence the structural architecture.

Beta East is structurally the simplest segment and is three-way dip closed with and up-thrown fault seal (Figure 2.7). Beta North-West is similar in trapping style, while Beta South-West relies on a downthrown fault seal towards the Beta North-West segment (Figure 2.8).

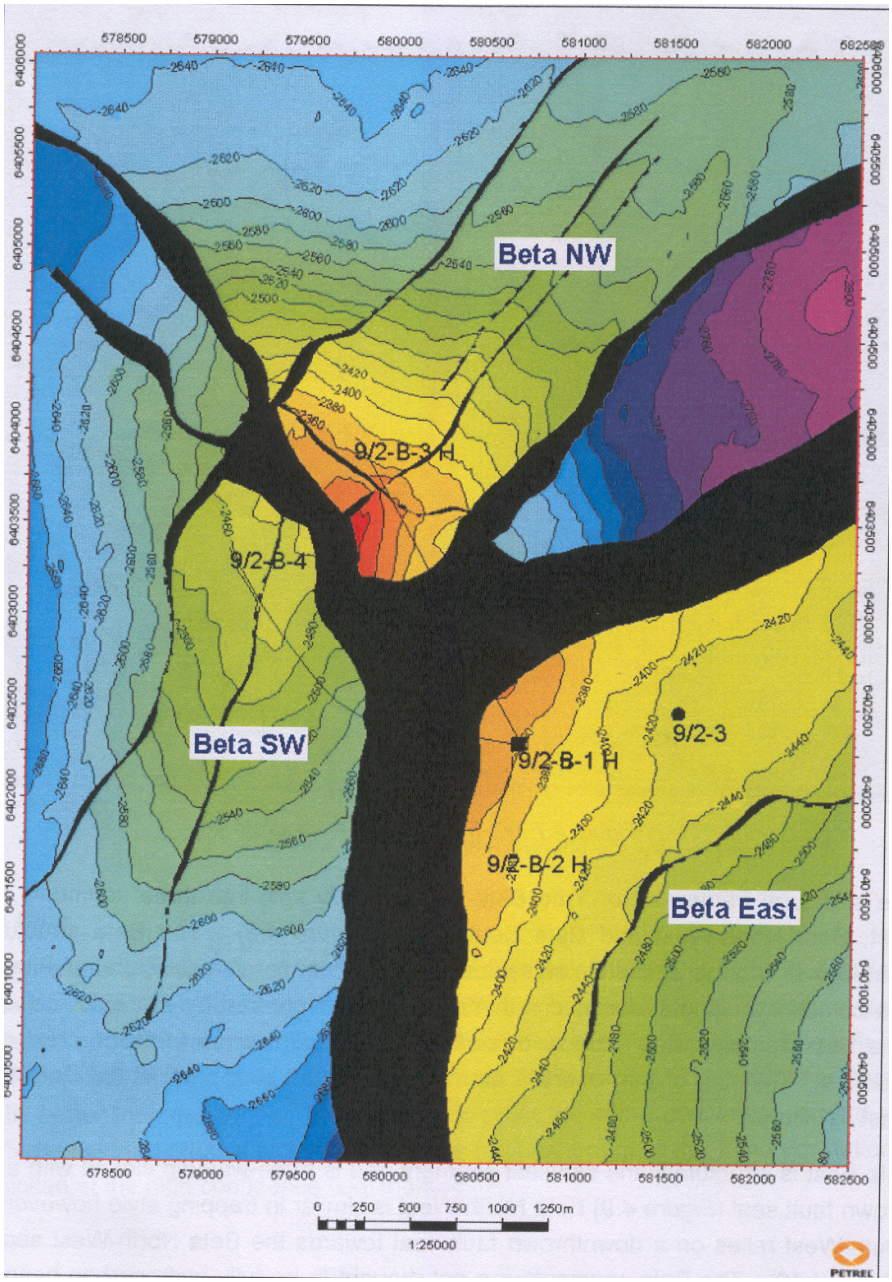

Figure 2.6: Beta Field Top Sandnes Formation TWT[1]

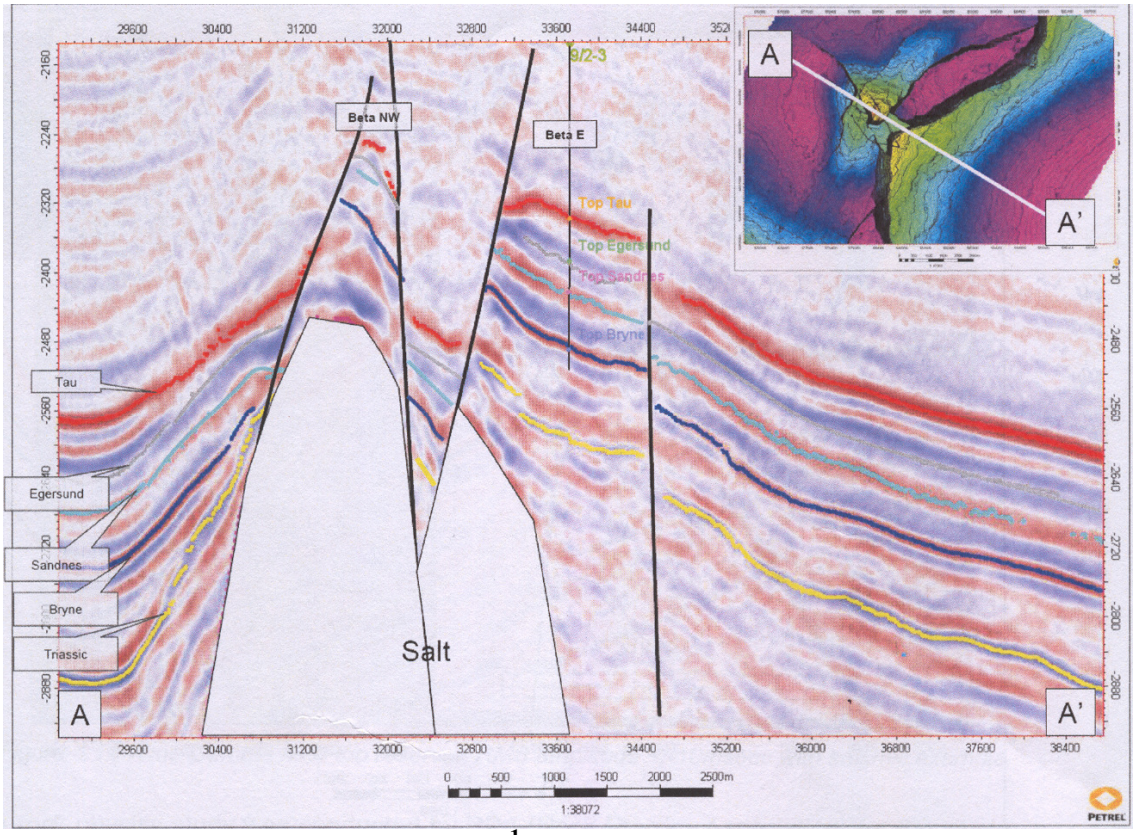

Figure 2.7: Beta East Seismic Section[1]

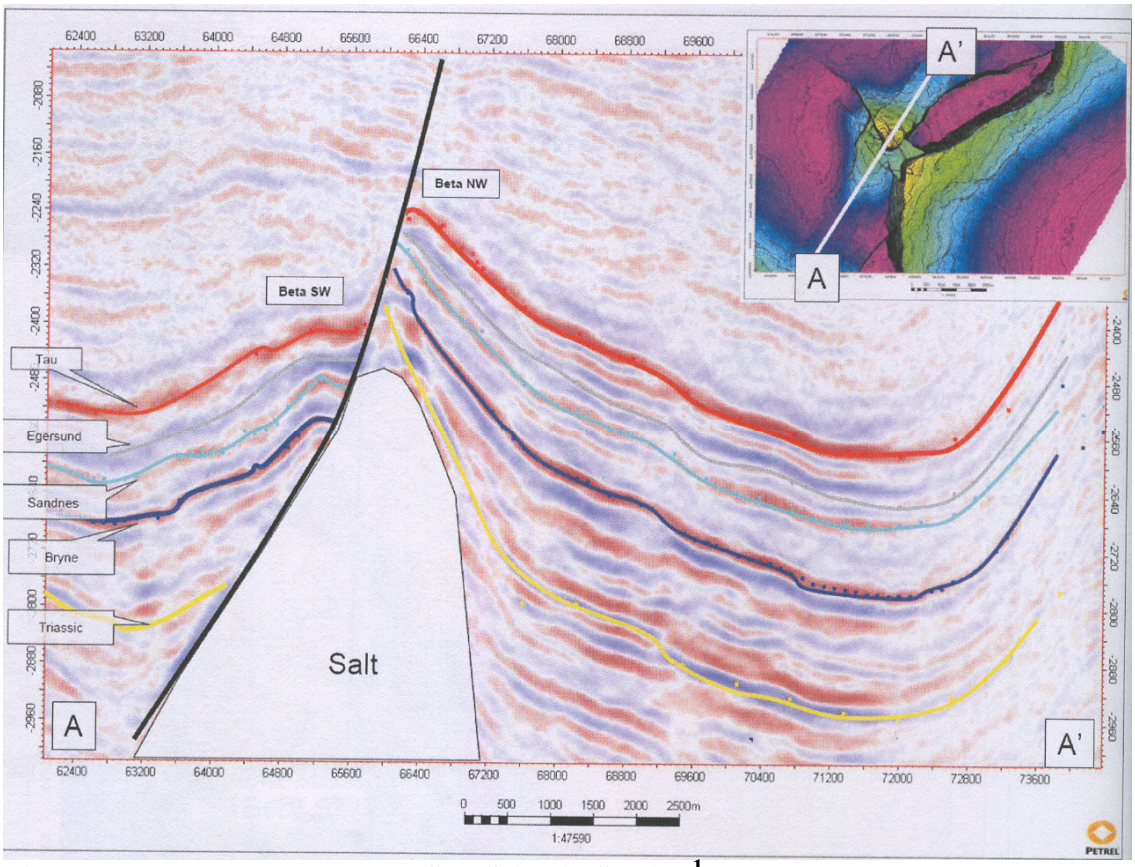

Figure 2.8: Beta NW and Beta SW Seismic Section[1]

2.4 Recovery and remaining reserves[1]

Statoil's production from the Gamma and Beta reservoirs up to shut down in May 2001, averaged around 6,500 Sm^3 o/d (40,000 bopd) for about two years before declining as water production increased. But sidetracking some wells in 1999 and 2000 resulted in significant gains.

Statoil recovered 5.6 $MMSm^3$ of oil (35MMstb) from Gamma and 2.5$MMSm^3$ (16MMstb) from Beta. Based on Statoil's calculation of STOIIP this resulted in recovery factors of 24% and 12% for Gamma and Beta respectively.

The Gamma West reservoir will now be drained by three highly deviated production wells, supported by two injection wells with simultaneous water and gas (SWAG) capability.
A fourth highly deviated production well will exploit the Gamma South-East reservoir.

In-field exploration potential exists in the un-drilled Gamma North-East block (STOIIP 3.2 $MMSm^3$ of oil (20MMstb)). It is planned to appraise Gamma North-East in the future, either as a sidetrack of a Gamma West well or as a new well from the production platform.

The Beta East reservoir will be drained by two highly deviated wells together with one water injection well. Beta North-West will be drained by one highly deviated production well and one water injection well. This well will be delayed by about three years due to higher risk associated with the Beta North-West reservoir.

Reservoir segment	Production to date MMSm3 (MMstb)	P50 STOIIP(*) MMSm3 (MMstb)	RF to date	Remaining Reserves (*)(**) MMSm3 (MMstb)	Expected Final RF
Gamma	5.6 (35)	28.5 (179)	20 %	5.7 (36)	40 %
Beta	2.5 (16)	24.6 (155)	10 %	4.8 (30)	29 %
Total	8.1(51)	53.1 (334)	15 %	10.5 (66)	35 %

Table 2.1: Recover Factors (RF) and Remaining Reserves[1]

(*) Note: STOIIP and remaining reserves excludes Gamma NE and Beta SW
(**) Note: Technical reserves assuming a field life to year 2023

3 Rock mechanics

Rock mechanics is different from solids mechanics. Generally we separate between homogeneity-heterogeneity and isotropy – anisotropy in materials. Homogeneity means that the properties are the same at different locations inside a material, whereas isotropic means the properties are the same in all directions. Conversely, heterogeneity means that properties vary from place to place, and anisotropic means that properties vary with direction[3]. Industrial materials are refined as homogeneous and isotropic, while rocks often are heterogeneous and anisotropic. For the purpose of simplification it is often assumed in rock mechanics that the material is homogeneous and isotropic.

3.1 Definition of stress

Stress is defined as average force acting over an area. This area may be a surface or an imaginary plane inside a material. In figure 3.1, a volume is loaded with a given force dF. The force is acting through any cross section of the volume. The area of the cross section is given as dA.

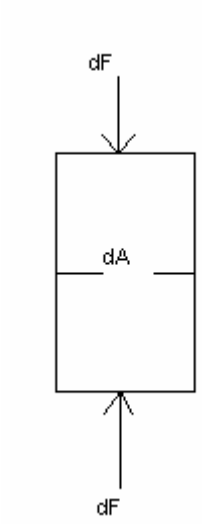

Figure 3.1: Force acting on a volume

The stress at the cross section is given by:

$$\sigma = \frac{dF}{dA} \tag{3.1}$$

Orientation of the cross section relative to the direction of the force is also important.
In figure 3.2 it is shown the forces acting on a surface.

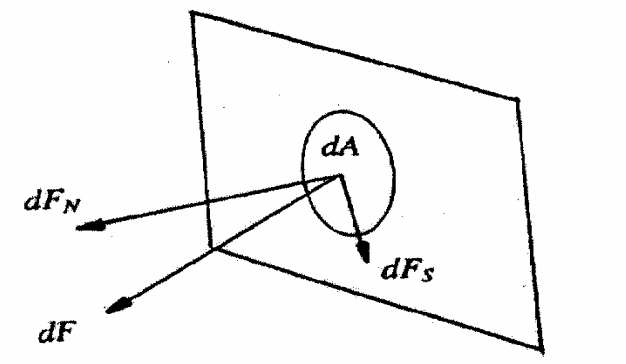

Figure 3.2: Forces acting on a surface[3]

The force is no longer normal to the cross section. We may then decompose the force into two components; dF_N that is normal to the cross section and dF_S that is parallel to the cross section. The normal stress and the shear stress can now be defined:

$$\sigma = \frac{dF_N}{dA} \qquad \text{and} \qquad \tau = \frac{dF_S}{dA} \tag{3.2}$$

In three dimensions we may define stress components which define all three dimensions. Figure 3.3 shows the stress state of a cube.

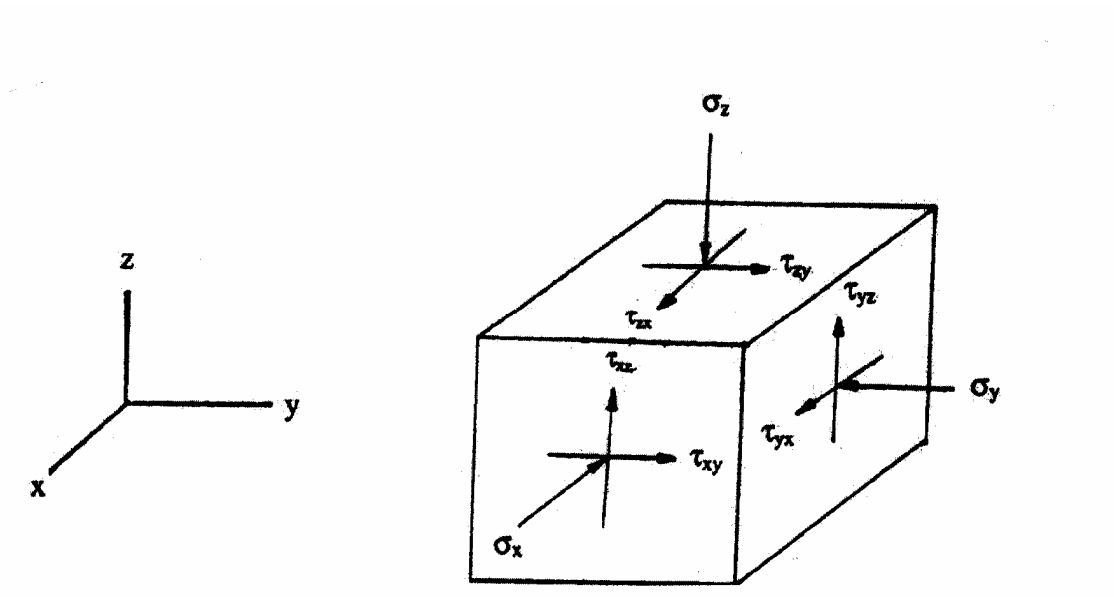

Figure 3.3: Stresses acting on the faces of a cube[3]

For a stressed body to remain at rest, it is required according to Newton's second law, that all forces acting on the body cancel each other out. Nine different components of stress are shown in the figure 3.3. These are:

Normal stresses: $\sigma_x, \sigma_y, \sigma_z$
Shear stresses: $\tau_{xy}, \tau_{yx}, \tau_{xz}, \tau_{zx}, \tau_{yz}, \tau_{zy}$

When assuming that the cube is at rest, no translational or rotational force is acting on it. This means we can put:

$\tau_{xy} = \tau_{yx}$
$\tau_{xz} = \tau_{zx}$
$\tau_{yz} = \tau_{zy}$

The stress tensor becomes:

$$[\sigma] = \begin{bmatrix} \sigma_x & \tau_{xy} & \tau_{xz} \\ \tau_{xy} & \sigma_y & \tau_{yz} \\ \sigma_{xz} & \tau_{yx} & \sigma_z \end{bmatrix} \tag{3.3}$$

The stress state can now be defined by three normal stresses and three shear stresses. In rock mechanics compressive stresses are usually defined as positive, while tensile stresses are negative.

3.2 Principal stresses

If we rotate the coordinate system to an orientation where all shear stresses vanishes, the normal stresses re defined as principal stresses.
The general definition of the principal stresses is:

$$[\sigma] = \begin{bmatrix} \sigma_x & \tau_{xy} & \tau_{xz} \\ \tau_{xy} & \sigma_y & \tau_{yz} \\ \tau_{xz} & \tau_{yz} & \sigma_z \end{bmatrix} = \begin{bmatrix} \sigma_1 & 0 & 0 \\ 0 & \sigma_2 & 0 \\ 0 & 0 & \sigma_3 \end{bmatrix} \tag{3.4}$$

If we move the right hand matrix over to the left and then taking the determinant, a solution for the principal becomes:

$$|0| = \begin{bmatrix} (\sigma_x - \sigma) & \tau_{xy} & \tau_{xz} \\ \tau_{xy} & (\sigma_y - \sigma) & \tau_{yz} \\ \tau_{xz} & \tau_{yz} & (\sigma_z - \sigma) \end{bmatrix} \tag{3.5}$$

The determinant of the equation must be calculated to find the principal stresses σ. The result will then be:

$$\sigma^3 - I_1\sigma^2 - I_2\sigma - I_3 = 0 \tag{3.6}$$

where:

$$\begin{aligned} I_1 &= \sigma_x + \sigma_y + \sigma_z \\ I_2 &= \tau_{xy}{}^2 + \tau_{xz}{}^2 + \tau_{yz}{}^2 - \sigma_x\sigma_y - \sigma_x\sigma_z - \sigma_y\sigma_z \\ I_3 &= \sigma_x\left(\sigma_y\sigma_z - \tau_{yz}{}^2\right) - \tau_{xy}\left(\tau_{xy}\sigma_z - \tau_{xz}\tau_{yz}\right) + \tau_{xz}\left(\tau_{xy}\tau_{yz} - \tau_{xz}\sigma_y\right) \end{aligned} \tag{3.7}$$

I_1, I_1 and I_3 are called invariants as they remain invariant for a given stress state regardless of the orientation of the coordinate system[3]. The roots are the principal stresses where: $\sigma_1 \geq \sigma_2 \geq \sigma_3$.

3.3 Average and deviatoric stresses

The total stress is equal to the average stress plus the deviatoric stress, and we separate the stress into these two components because many failure mechanisms are governed by the deviatoric stress. This is due to the deviatoric stress reflects the shear stress level.

The average stress is defined as:

$$\sigma_m = \frac{1}{3}\left(\sigma_x + \sigma_y + \sigma_z\right) \tag{3.8}$$

The deviatoric stress is defined as:

$$[\sigma]_{dev} = \begin{bmatrix} (\sigma_x - \sigma_m) & \tau_{xy} & \tau_{xz} \\ \tau_{xy} & (\sigma_y - \sigma_m) & \tau_{yz} \\ \tau_{xz} & \tau_{yz} & (\sigma_z - \sigma_m \end{bmatrix} \tag{3.9}$$

The total stress will then be defined as:

$$[\sigma] = \begin{bmatrix} \sigma_x & \tau_{xy} & \tau_{xz} \\ \tau_{xy} & \sigma_y & \tau_{yz} \\ \tau_{xz} & \tau_{yz} & \sigma_z \end{bmatrix} = \begin{bmatrix} \sigma_m & 0 & 0 \\ 0 & \sigma_m & 0 \\ 0 & 0 & \sigma_m \end{bmatrix} + \begin{bmatrix} (\sigma_x - \sigma_m) & \tau_{xy} & \tau_{xz} \\ \tau_{xy} & (\sigma_y - \sigma_m) & \tau_{yz} \\ \tau_{xz} & \tau_{yz} & (\sigma_z - \sigma_m \end{bmatrix} \tag{3.10}$$

The principal deviatoric stresses are found by determining the eigenvalues of the matrix in the equation 3.9.

The total stress describes changes in volume and shape. The average stress is the same as hydrostatic stress, which may cause volume change in the body, but no shape change. The deviatoric components causes shape change, and give therefore rise to shear stresses[3].

3.4 Effective stresses

Rocks are usually porous material, which consist of a rock matrix and a fluid that's under pressure.

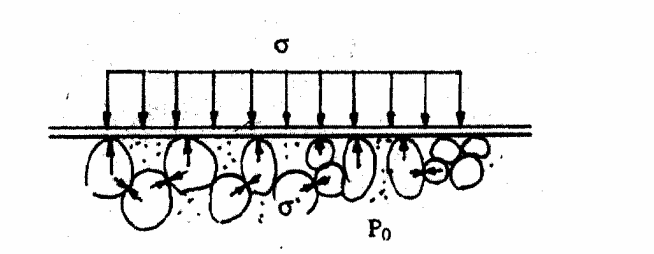

Figure 3.4: Stress and pressure in a porous material[3]

In figure 3.4 it's assumed a porous rock which is sealed by a plate. On the outside of the plate is a stress σ acting, inside there are stresses that must balance the outside stresses, in order for equilibrium to exist. This means that the stress inside the plate is partially taken up by the rock matrix and partially by the pore fluid. The total stress is then equal to the pore pressure plus the effective stress:

$$\sigma = \sigma' + P_o \quad \rightarrow \quad \sigma' = \sigma - P_o \tag{3.11}$$

A more general formulation of the effective stress includes a scaling factor in front of the pressure term. This is called the Biot's constant, β.

The equation will now become:

$$\sigma' = \sigma - \beta P_o \tag{3.12}$$

where:

$$\beta = \left(1 - \frac{E}{E_i}\frac{1-2\nu_i}{1-2\nu}\right) \tag{3.13}$$

Here E is the Youngs modulus, ν is the Poisson's ratio and i refers to the interpore material. The Biot's constant varies from 0.8 – 1 for real rocks.

Fluids can not transmit shear stresses, which mean that effective stresses are only valid for normal stresses. Shear stresses remain unchanged.

4 Stresses in a borehole

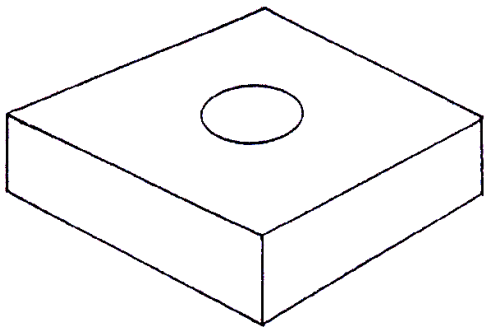

Figure 4.1: Basic hole in plate model[3]

This plate represent the rock formation, initial there is no hole. The plate is loaded on all sides, and has a uniform stress in each direction. This stress state is then called in-situ stress state. When we drill a hole in the middle of the plate, the stress state around the hole will change. This is because of the new geometrical element. The stress state around the hole is called a stress concentration. So we will deal with two categories of stresses:

- The in-situ stresses or the rock stresses
- The stresses around the hole

The Kirsch equations are very central in nearly all work related to rock mechanics.

4.1 The Kirsch equations[3]

$$\sigma_r = \frac{1}{2}(\sigma_x + \sigma_y)\left(1 - \frac{a^2}{r^2}\right) + \frac{1}{2}(\sigma_x - \sigma_y)\left(1 + 3\frac{a^4}{r^4} - 4\frac{a^2}{r^2}\right)\cos 2\theta + \tau_{xy}\left(1 + 3\frac{a^4}{r^4} - 4\frac{a^2}{r^2}\right)\sin 2\theta + \frac{a^2}{r^2}p_w$$

$$\sigma_\theta = \frac{1}{2}(\sigma_x + \sigma_y)\left(1 + \frac{a^2}{r^2}\right) - \frac{1}{2}(\sigma_x - \sigma_y)\left(1 + 3\frac{a^4}{r^4}\right)\cos 2\theta - \tau_{xy}\left(1 + 3\frac{a^4}{r^4}\right)\sin 2\theta - \frac{a^2}{r^2}p_w$$

$$\sigma_z = \sigma_{zz} - 2\nu(\sigma_x - \sigma_y)\frac{a^2}{r^2}\cos 2\theta - 4\nu\tau_{xy}\frac{a^2}{r^2}\sin 2\theta \qquad (4.1)$$

$$\tau_{r\theta} = \left\{\frac{1}{2}(\sigma_x - \sigma_y)\sin 2\theta + \tau_{xy}\cos 2\theta\right\}\left(1 - 3\frac{a^4}{r^4} + 2\frac{a^2}{r^2}\right)$$

$$\tau_{rz} = \left\{\tau_{xz}\cos\theta + \tau_{yz}\sin\theta\right\}\left(1 - \frac{a^2}{r^2}\right)$$

$$\tau_{\theta z} = \left\{-\tau_{xz}\cos\theta + \tau_{yz}\sin\theta\right\}\left(1 + \frac{a^2}{r^2}\right)$$

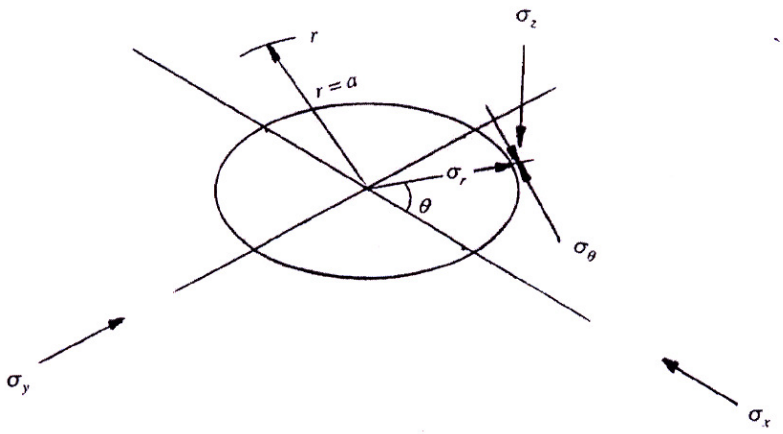

Figure 4.2: Stresses acting on the borehole wall[3]

Where: a – radius of the hole
r – position radially outwards from the center
θ – angle with the direction of the maximum horizontal stress
ν – Poisson's ratio

Now we have an expression for the borehole wall, or the stress state in the adjacent formation.

At the borehole wall (r=a), the equations are reduced to:

Radial stress: $\sigma_r = P_w$

Tangential stress: $\sigma_\theta = \sigma_x + \sigma_y - P_w - 2(\sigma_x - \sigma_y)\cos(2\theta) - 4\tau_{xy}\sin(2\theta)$

Axial stress, plane strain: $\sigma_z = \sigma_{zz} - 2\gamma(\sigma_x - \sigma_y)\cos(2\theta) - 4\mu\tau_{xy}\sin(2\theta)$ (4.2)

Axial stress, plane stress: $\sigma_z = \sigma_{zz}$

Shear stress: $\tau_{\theta z} = 2(\tau_{yz}\cos\theta - \tau_{xz}\sin\theta)$

$\tau_{rz} = \tau_{r\theta} = 0$

These equations are the most important equations in applied rock mechanics.

4.2 Stresses in three dimensions

In the Kirsch equations, one often assumes a horizontal and vertical in-situ stress field. The borehole may assume any orientation. Then we have to define equations to transform the in-situ stresses to the orientation of the borehole. In the oil industry it is common to assume three principle in-situ stresses, the vertical or overburden stress σ_v, and the maximum and minimum horizontal stresses, σ_H and σ_h. Figure 4.3 shows the most important stresses. The input stresses are the in-situ stresses σ_v, σ_H and σ_h. Since the borehole may assume any orientation, these stress must be transformed into a new coordinate system x, y and z. And we look at the stresses as σ_x, σ_y and σ_z .The directions of the new stress components are given by the borehole inclination from vertical γ, the geographical azimuth ϕ and the borehole position from the x-axis, θ.

The following equations define all transformed stress components shown in figure 4.3.

$$\sigma_x = \left(\sigma_H \cos^2\phi + \sigma_h \sin^2\phi\right)\cos^2\gamma + \sigma_v \sin^2\gamma$$

$$\sigma_y = \left(\sigma_H \sin^2\phi + \sigma_h \cos^2\phi\right)$$

$$\sigma_{zz} = \left(\sigma_H \cos^2\phi + \sigma_h \sin^2\phi\right)\sin^2\gamma + \sigma_v \cos^2\gamma \qquad (4.3)$$

$$\tau_{yz} = \frac{1}{2}\left(\sigma_h - \sigma_H\right)\sin(2\phi)\sin\gamma$$

$$\tau_{xz} = \frac{1}{2}\left(\sigma_H \cos^2\phi + \sigma_h \sin^2\phi - \sigma_v\right)\sin(2\gamma)$$

$$\tau_{xy} = \frac{1}{2}\left(\sigma_h - \sigma_H\right)\sin(2\phi)\cos\gamma$$

All equations are now defined which are enquired to analyze failures of boreholes.

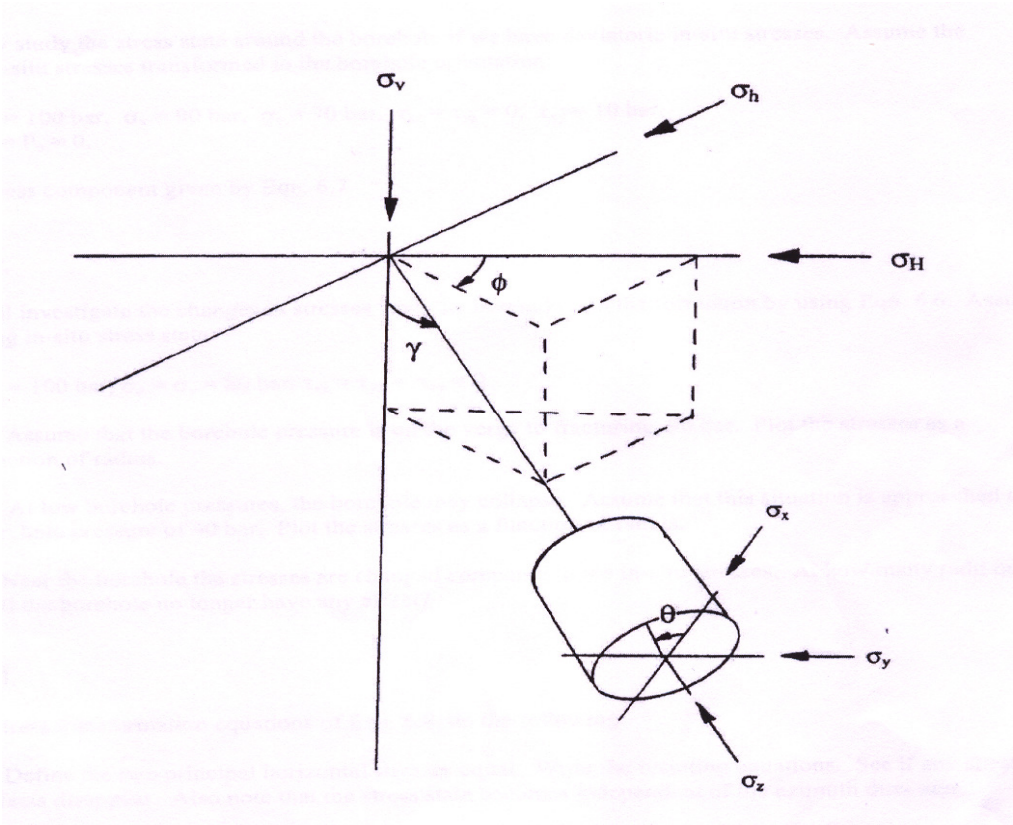

Figure 4.3: In-situ stresses, the transformed stresses and their relative orientation[3]

5 Failure criterions

Below, two different failure criterions are presented:

- The Von Mises shear strength
- The Mohr-Coulomb shear model

5.1 Von Mises shear strength

The definition of the second deviatoric invariants is used to construct the von Mises shear diagram. The second deviatoric stress invariant is found by replacing the normal stress components in equation with the difference between the normal and average stresses.

Equation 3.6 is defined as:

$$\sigma^3 - I_1\sigma^2 - I_2\sigma - I_3 = 0 \tag{5.1}$$

where:

$$\begin{aligned} I_1 &= \sigma_x + \sigma_y + \sigma_z \\ I_2 &= \tau_{xy}{}^2 + \tau_{xz}{}^2 + \tau_{yz}{}^2 - \sigma_x\sigma_y - \sigma_x\sigma_z - \sigma_y\sigma_z \\ I_3 &= \sigma_x\left(\sigma_y\sigma_z - \tau_{yz}{}^2\right) - \tau_{xy}\left(\tau_{xy}\sigma_z - \tau_{xz}\tau_{yz}\right) + \tau_{xz}\left(\tau_{xy}\tau_{yz} - \tau_{xz}\sigma_y\right) \end{aligned} \tag{5.2}$$

$$\sigma_1 \rangle \sigma_2 \rangle \sigma_3$$

The second deviatoric stress invariant becomes:

$$J_2^{1/2} = \sqrt{\frac{1}{6}\left[(\sigma_1 - \sigma_2)^2 + (\sigma_2 - \sigma_3)^2 + (\sigma_3 - \sigma_1)^2\right]} \tag{5.3}$$

This is plotted against the normal effective stress invariant, equation 5.4.

$$\sigma_m - P_o = \frac{1}{3}(\sigma_1 + \sigma_2 + \sigma_3) - P_o \tag{5.4}$$

The line in the diagram is a failure line, which means that the stress state above the line defines an intact material, and stress state below the line is defined as failure. Figure 5.1 below gives an example of a von Mises diagram.

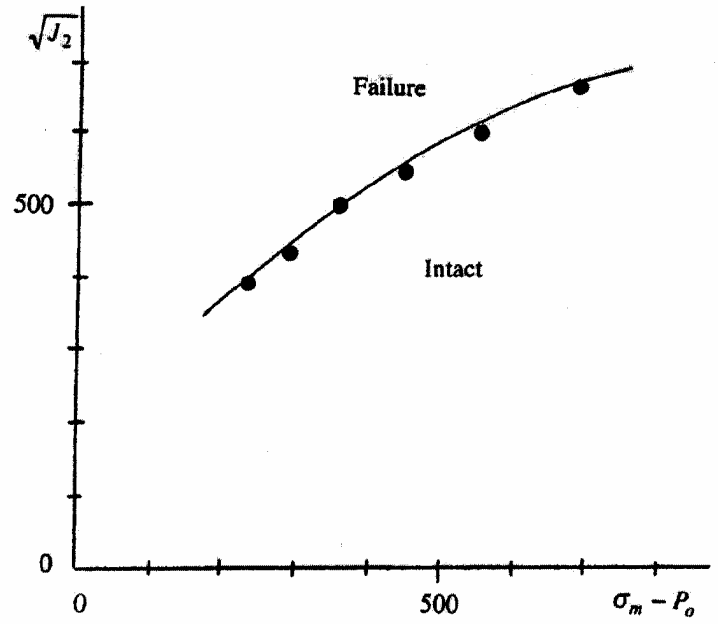

Figure 5.1: von Mises failure envelope from triaxial test data[3]

5.2 The Mohr-Coulomb shear model

First we have to define Mohr's circle. The Mohr's circles are found as shown in the figure 5.2 below.

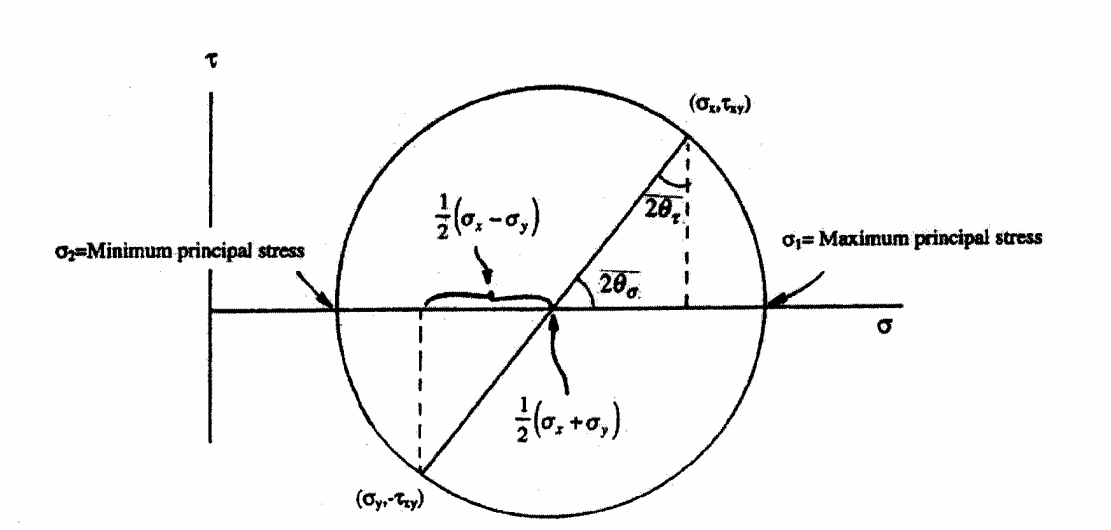

Figure 5.2: Mohr's circle[3]

The Mohr-Coulomb shear model uses several Mohr's circles in a σ'τ-plot (Figure5.3)

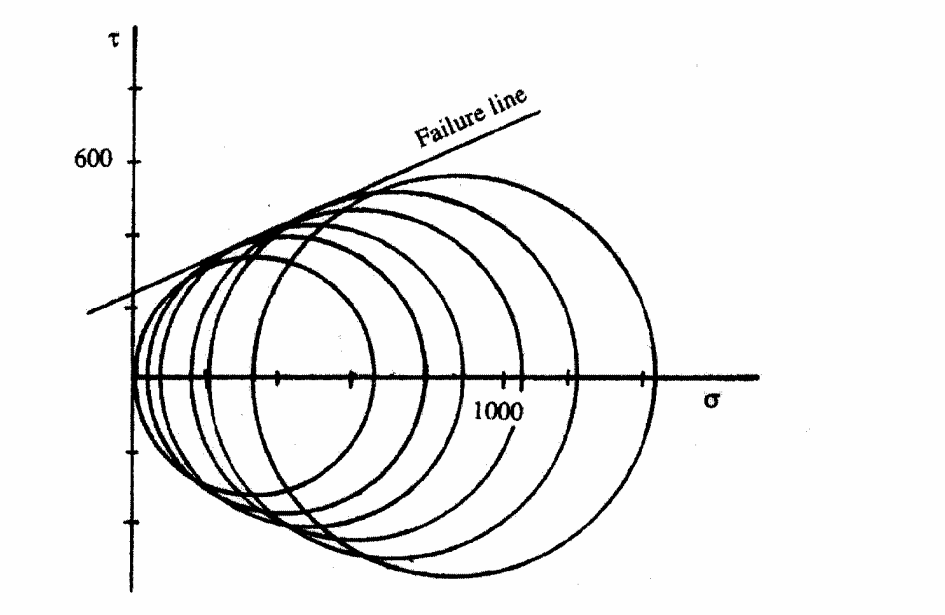

Figure 5.3: Mohr-Coulomb failure model[3]

After constructing the circles which represent the stress state at failure, a failure line is drawn, which represent the stress state at failure. When a stress circle crosses the failure line, failure occurs. The Mohr-Coulomb failure model is this failure line, which can be expressed as:

$$\tau = \tau_0 + \sigma' \tan\phi \qquad (5.5)$$

Here τ_0 is the cohesion, ø is the angle of internal friction and σ' is the effective normal stress. The parameters are shown in figure 5.4.

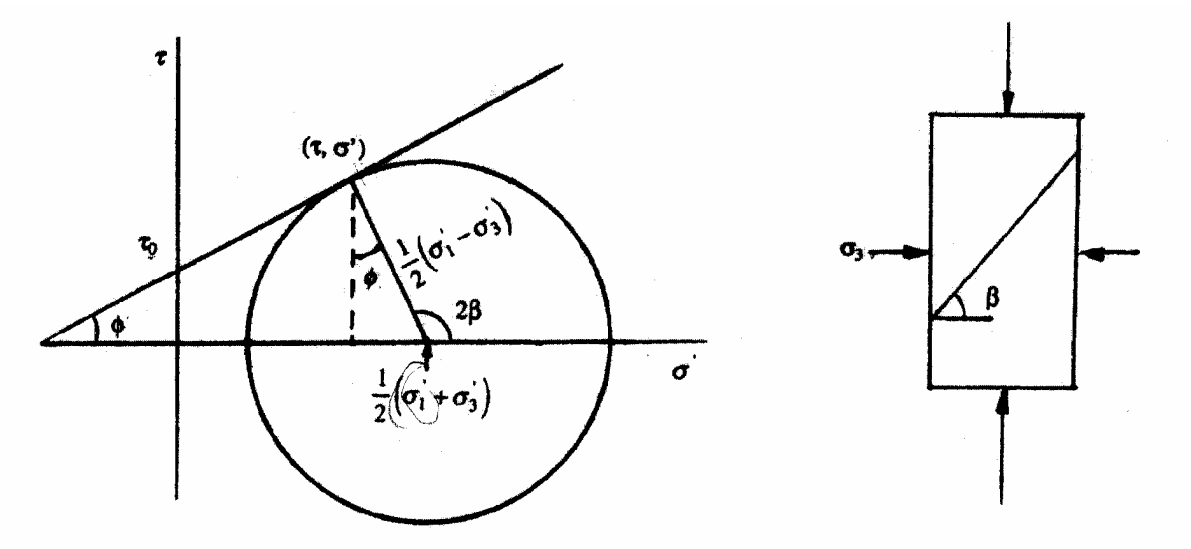

Figure 5.4: Stresses at failure for the Mohr-Coulomb failure model[3]

Inspection of the figure 5.4 reveals that the coordinates (τ, σ') at failure is defined by the following equations:

$$\tau = \frac{1}{2}(\sigma'_1 - \sigma'_3)\cos\phi$$

$$\sigma' = \frac{1}{2}(\sigma'_1 + \sigma'_3) - \frac{1}{2}(\sigma'_1 - \sigma'_3)\sin\phi \tag{5.6}$$

Inserting equation 5.6 into equation 5.5, defines the stress state at failure. This result in:

$$\frac{1}{2}(\sigma'_1 - \sigma'_3)\cos\phi = \tau_0 + \left[\frac{1}{2}(\sigma'_1 + \sigma'_3) - \frac{1}{2}(\sigma'_1 - \sigma'_3)\sin\phi\right]\tan\phi \tag{5.7}$$

The fracture angle on the plug shown in figure can be determined from the following expression:

$$\beta = 45° + \frac{\phi}{2} \tag{5.8}$$

6 Fracturing data

There are several ways to determine the fracturing pressure of a formation. Amongst these are Leak-Off test (LOT), Extended Leak-off test (ELOT) and Formation Integrity test (FIT). Extended Leak-off test yields the best estimate of the in-situ stress. Leak-off test may yield satisfactory results, whereas Formation Integrity test only give a vague indication[5].

6.1 Leak-off test[6]

A test to determine the strength or fracture pressure of the open formation, usually conducted immediately after drilling below a new casing shoe. During the test, the well is shut in and fluid is pumped into the wellbore to gradually increase the pressure that the formation experiences. At some pressure, fluid will enter the formation, or leak off, either moving through permeable paths in the rock or by creating a space by fracturing the rock. The results of the leak-off test dictate the maximum pressure or mud weight that may be applied to the well during drilling operations. To maintain a small safety factor to permit safe well control operations, the maximum operating pressure is usually slightly below the leak-off test result. A typical leak-off test would give a pressure diagram like the one shown in figure 6.1.

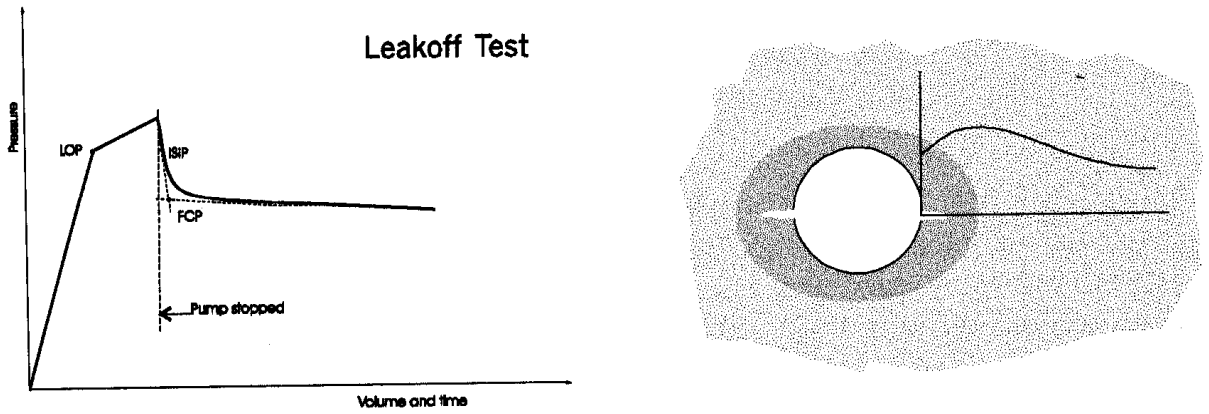

Figure 6.1: The pressure diagram and the effects on the formation of an LOT[5]

Because the stress state increases with depth, the leak-off pressures also typically increases with depth.

6.2 Extended leak-off test

When additional or more accurate information about the in-situ stress is needed, the extended leak-off test is used. The procedure is similar to the LOT, but the pumping continues after the leak-off point is reached. This is to make sure that the fracture has propagated in to undisturbed formation[5]. A typical extended leak-off test would give a pressure diagram like the one shown in figure 6.2.

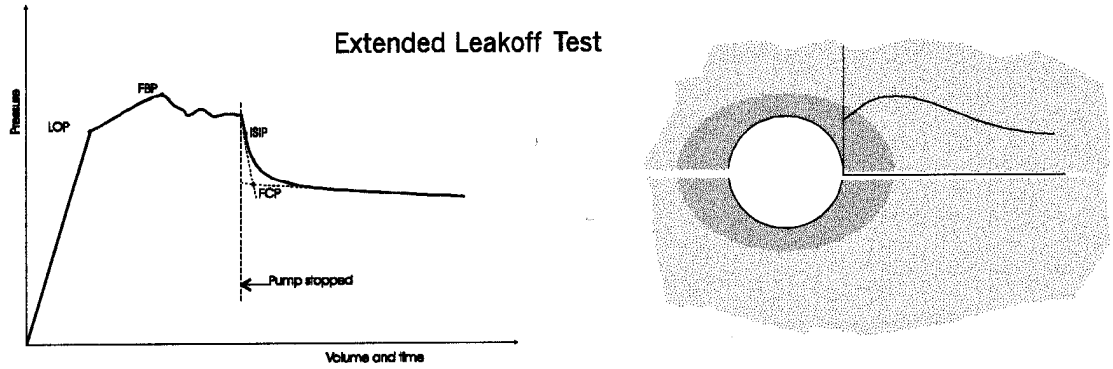

Figure 6.2: The pressure diagram and the effect on the formation of an ELOT[5]

6.3 Formation integrity test

Leak-off tests are not performed all wells today. The reason for this is that most new wells are drilled with oil based mud in the lower sections of the well. This type of mud s very expensive and during a leak-off test, a large volume of mud is lost. Oil based mud also gives a poor repair of the fractures. For this reason, in most wells drilled with oil based mud, only a FIT s performed. In the FIT the formation is not fractured. The purpose of the test is to test the formation to see if it can withstand the mudweight planned for the next hole section. The pressure is increased in the same way as for LOT, but the pumps are stopped when a predetermined value below the leak-off pressure is reached. The well is shut in and pressure versus volume is recorded. FIT have little or no use in measuring stresses, because a leak-off or breakdown of the formation is not achieved. A typical FIT would give a pressure diagram shown in figure 6.3.

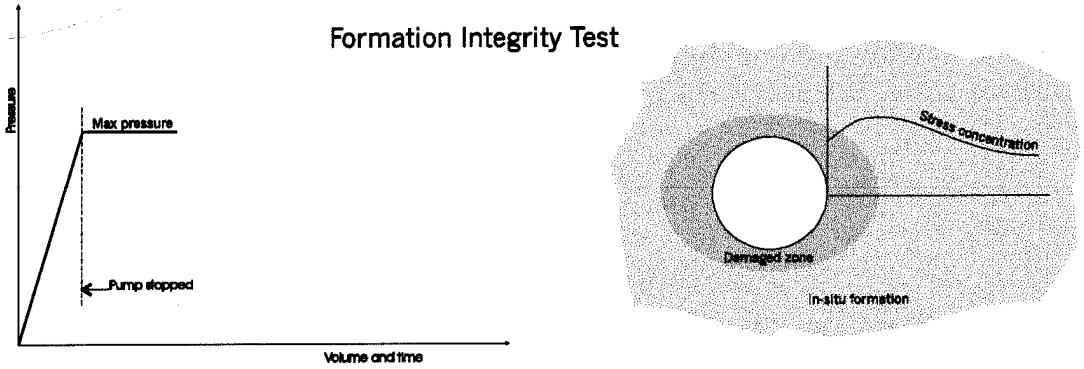

Figure 6.3: Pressure diagram and the effect on the formation of a FIT[5]

7 Normalizing of the fracture data

It is known that the leak-off data vary for no obvious reasons. This is due to other lateral variation and anisotropy in the in-situ stress field. The reason for the normalization process is to reduce the spread in the raw data and discover hidden trends. The two most used normalization methods are to normalize for different borehole inclinations and to use the compaction model.
These two models are presented in the following.

7.1 Normalizing for different borehole inclination

From rock mechanics it is known that the fracture gradient may depend on the inclination and azimuth of the boreholes. This effect is mainly dependent on the relative magnitudes of the three principal in-situ stresses. Here we assume a relaxed depositional environment, meaning an isotropic in-situ stress field. A method for modelling an anisotropic case is presented later in chapter 9. We can express the fracture gradient in terms of stresses on the borehole wall:

$$P_{wf} = 3\sigma_y - \sigma_x - P_0 \tag{7.1}$$

The stress components can further be expressed with the assumption from Aaadøy & Chenevert[4] as:

$$\begin{aligned} \sigma_x &= \sigma_a \cos^2\gamma + \sigma_v \sin^2\gamma \\ \sigma_y &= \sigma_a \end{aligned} \tag{7.2}$$

If we combine the expressions above, we may obtain and expression for the fracture gradient for any inclination as:

$$P_w = 2\sigma_a - P_o - (\sigma_v - \sigma_a)\sin^2\gamma \tag{7.3}$$

We assume that we have fracture data for inclined boreholes, which we want to make comparable by calculating the equivalent fracture gradient for a vertical hole. By setting up two equations (equation 7.3) one for an inclined hole and one for a vertical hole and then combining these, the result become:

$$P_{wf}(0) = P_{wf}(\gamma) + (\sigma_v - \sigma_a)\sin^2\gamma \tag{7.4}$$

In the equation above we need an estimate for the average horizontal stress, but setting up an equation for the fracturing of a vertical hole, the horizontal stress can be eliminated in the equation above. The result will now be:

$$P_{wf}(0) = P_{wf}(\gamma) + \frac{\left(\sigma_v - \frac{1}{2} P_o\right)\sin^2\gamma}{1 + \frac{1}{2}\sin^2\gamma} \tag{7.5}$$

This is the final equation.

7.2 The compaction model

The compaction model is a method to estimate changes in the fracturing pressures due to the depletion of pore pressure in a reservoir. The model normalizes the leak-off data to the same pore pressure. If the pore pressure has changed over time, we can estimate what effect this have on the fracturing pressure. If the data shows a trend, it is likely that the pore pressures have the same origin, but have been altered in resent time due to geological processes or production.

When the pore pressure is lowered as a consequence of depletion and the overburden remains constant, some of the load held by the initial pore pressure is transferred to the rock matrix. The increased vertical matrix stress will via the Poisson's also increase the horizontal stress. Assuming that the overburden stress remains constant, and that no strain is allowed on the sides of the rock, Aadnøy[2] has delivered a simple model with reference to pore pressure history. The effect over time of a change pore pressure on the fracturing pressure is given by equation 7.6.

$$\Delta P_{wf} = \Delta P_o \frac{1-3\nu}{1-\nu} \tag{7.6}$$

Where ΔP_{wf} is the corresponding change in fracturing pressure, ΔP_o is the change is pore pressure and ν is the Poisson's ratio. Figure 7.1 under, shows the principal of the compaction model.

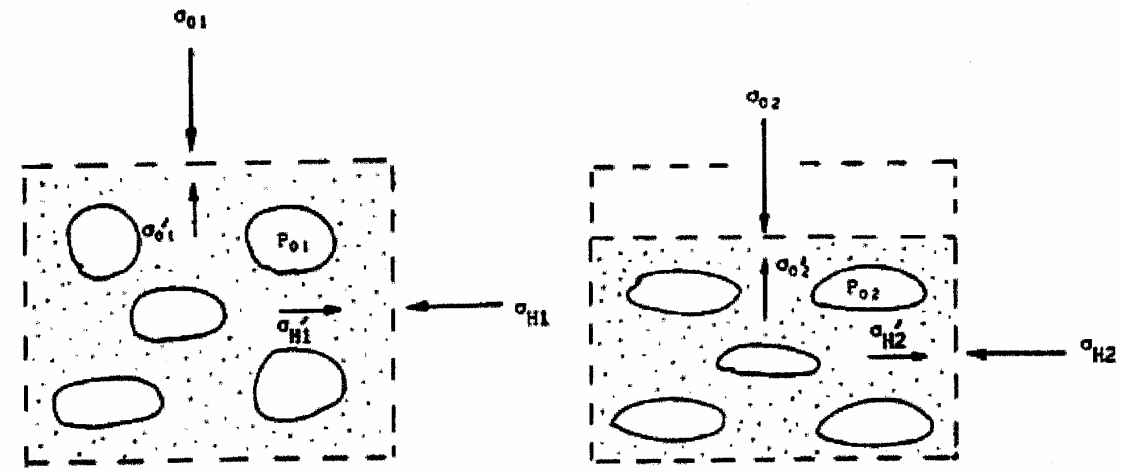

Figure 7.1: Illustration of the compaction model with the initial pore pressure and with reduced pore pressure[2]

8 Geological aspects

One often separate between two different geological aspects, a relaxed depositional environment also know as an isotropic stress field and an anisotropic stress field.
In the following the difference between the two are presented.

In a relaxed depositional environment we often neglect tectonic effects, and assume that the horizontal in-situ stress field is due to rock compaction only[3]. An isotropic stress field implies the same horizontal stresses in all directions. If deviated boreholes are drilled, there are no directional abnormalities for the same wellbore inclination and the same leak-off value is expected in all geographical directions. Since the horizontal stresses in a relaxed depositional environment are lower than the overburden stress, the fracture gradient will decrease with the hole angle, this is shown in figure 8.1 under. By estimating a constant horizontal stress gradient for the field, the situation is relatively simple to analyse. But an ideal stress situation is rarely the case, usually a more complex stress situation exists.

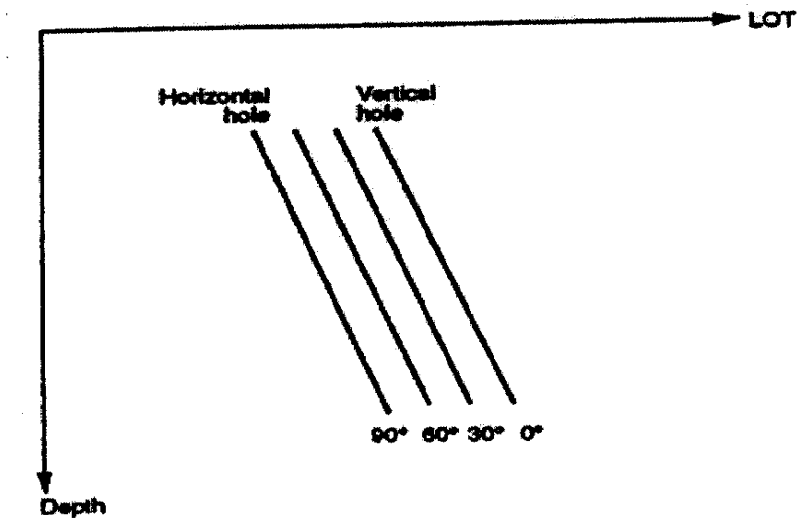

Figure 8.1: Expected leak-off behaviour, relaxed depositional environment[3]

In an anisotropic stress field the horizontal stress field usually varies with the direction and we have two different principal stresses. An anisotropic may be caused by global geologic processes as plate tectonics, or due to local effects like salt domes, topography or faults. The resulting stress state varies over the area. Figure 8.2 shows the Yme field. One observation is that there is a considerable spread in the leak-off data.

It is obvious that the Yme field is an anisotropic stress field. The experience is that most oil fields exhibit anisotropic stress field to some degree[3].

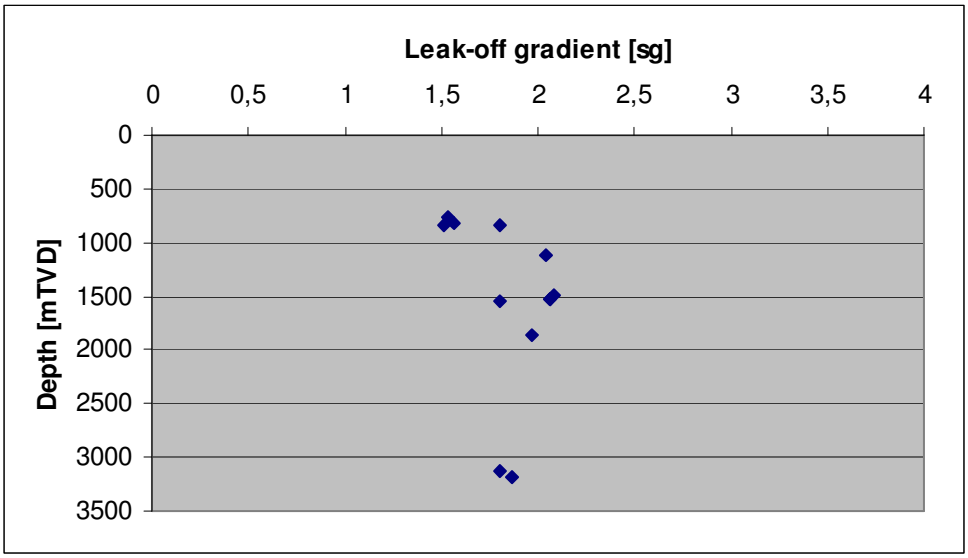

Figure 8.2: Yme leak-off data vs. depth

In chapter 9, a method for modelling an anisotropic stress field is presented. The method is called the inversion technique.

9 The Inversion Technique

From earlier we have found that the field is an anisotropic field, the best way to modelling the field from fracturing data is to use the inversion technique. The inversion technique is a unique modelling method developed by Aadnøy[2+3]. The technique uses leak-off data to predict stresses in the formation, and also predicts fracturing pressures for new wells.

The field data used as input for the method includes the leak off pressure, depth, pore pressure, overburden stress, inclination and azimuth for each data point.

Where the following definition relates to the inversion technique:

γ is the inclination of the wellbore at the casing shoe.
φ is the azimuth angle of the wellbore clockwise from north
β is the angle from north to the maximum horizontal stress
σ_H is the estimated maximum horizontal stress
σ_h is the estimated minimum horizontal stress

The figure 9.1 under illustrates the method. When we have two or more data sets, the inversion technique will calculate the horizontal stress that fits all data sets.

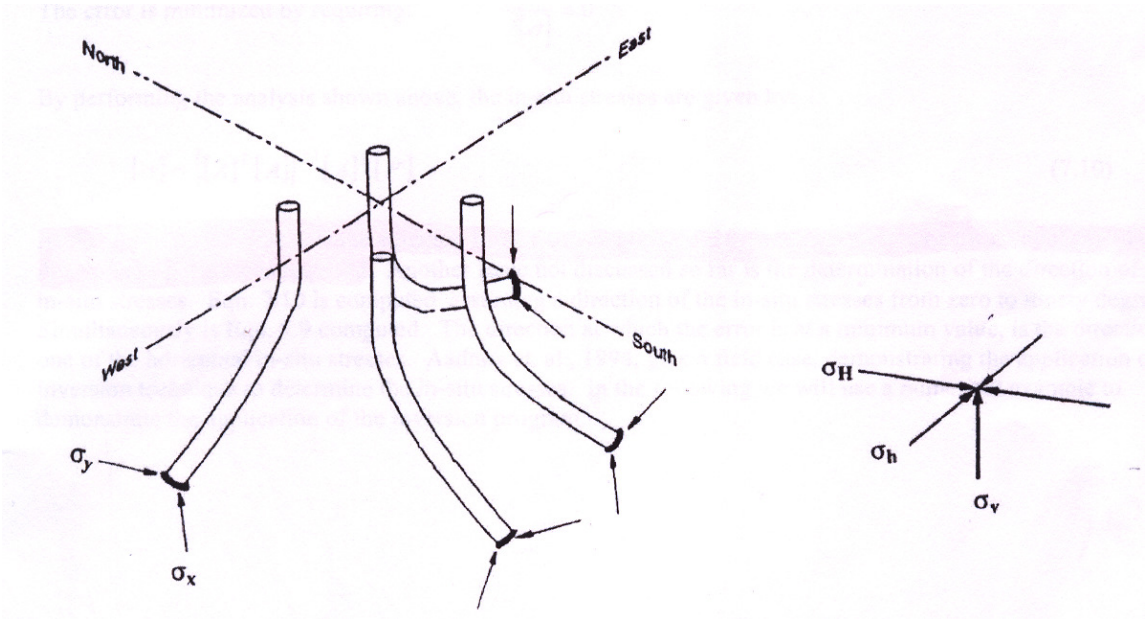

Figure 9.1: Stresses acting on inclined boreholes are transformed from the in-situ stress field[3]

Aadnøy & Chenevert derived from the Kirsch equations in chapter 4, a relationship for the fracture pressure of a borehole when $\sigma_x > \sigma_y$, assuming no shear stresses at the borehole wall. This relationship is given by equation 9.1:

$$P_{wf} = 3\sigma_y - \sigma_x - P_0 + \sigma_t \qquad \text{for } \sigma_y < \sigma_x \qquad (9.1)$$

The two normal stresses is then replaced by the transformation equations, given here by equation 9.2:

$$\begin{aligned} \sigma_x &= \left(\sigma_H \cos^2\phi + \sigma_h \sin^2\phi\right)\cos^2\gamma + \sigma_v \sin^2\gamma \\ \sigma_y &= \left(\sigma_H \sin^2\phi + \sigma_h \cos^2\phi\right) \end{aligned} \qquad (9.2)$$

By inserting equation 9.2 into equation 9.1, the dividing by the overburden and rearranging the result, equation 9.3a becomes the outcome:

$$\frac{P_{wf} + P_o}{\sigma_v} + \sin^2\gamma = \left(3\sin^2\phi - \cos^2\phi\cos^2\gamma\right)\frac{\sigma_k}{\sigma_v} + \left(3\cos^2\phi - \sin^2\phi\cos^2\gamma\right)\frac{\sigma_l}{\sigma_v} \qquad (9.3a)$$

Or in short form:

$$P' = a\frac{\sigma_k}{\sigma_v} + b\frac{\sigma_l}{\sigma_v} \qquad (9.3b)$$

The two equations have two unknowns, the horizontal in-situ stresses, called σ_k and σ_l. When we have data sets from two well sections with different orientation, one can determine the two unknown stresses. The largest stress is redefined to σ_H and the smallest to σ_h.

If there are observations from several different wells, equation can be used to construct a system of equations that in matrix from look like equation 9.4a.

$$\begin{bmatrix} P_1 \\ P_2 \\ P_3 \\ .. \\ P_n \end{bmatrix} = \begin{bmatrix} a_1, b_1 \\ a_2, b_2 \\ a_3, b_3 \\ .., .. \\ a_n, b_n \end{bmatrix} \begin{bmatrix} \sigma_k/\sigma_v \\ \sigma_l/\sigma_v \end{bmatrix} \qquad (9.4a)$$

Or

$$[P'] = [A][\sigma] \qquad (9.4b)$$

At least two measurements are needed to solve the equation. Where there are more observations than unknowns the system becomes overdetermined. In an overdetermined system there will always be an error. To solve for this, the error between the model and he measurement is:

$$[e] = [A][\sigma] - [P'] \tag{9.5}$$

This error will be minimized by using the least squares method, which gives this equation:

$$[e^2] = [e]^T [e] \tag{9.6}$$

The error is minimized by requiring:

$$\frac{\partial e^2}{\partial [\sigma]} = 0 \tag{9.7}$$

By performing the analysis shown above, the in-situ stresses are given by:

$$[\sigma] = \left\{ [A]^T [A] \right\}^{-1} [A]^T [P'] \tag{9.8}$$

We can see that the equation 9.8 is too cumbersome for manual calculation, so the use of computer programme makes the calculation a lot easier. The direction of the in-situ stress field also ha to be determined. This is done by assuming a direction of the in-situ stresses to be between zero and ninety degrees. By plotting the squared error from the equation 9.6 as a function of the angle, the direction is given from the point in the graph where the error is at the minimum value.

10 Borehole stability

Borehole stability can cause problems in any drilling operations. Stability problems can result in lost time and sometimes also loss of equipment which means extra cost.
Stability problems can appear in both vertical and horizontal well. Long-reach deviate wells are specially known for having problems with the stability.

Stability evaluation of a well represents a classical rock mechanics problem: prediction of a rock's response to mechanical loading[7].
Evaluation of the borehole stability is often very difficult. Here are some special circumstances that make evaluation of stability problematic[7]:

- The drill bit may be several thousand of meters away, and there are no methods available for direct observation of what is happening.

- There may be large variations in formation stresses, and in-situ stresses are not measured systematically

- There are large variations in the material properties of the formations. Coring costs are high, and only limited amounts of material are available for rock mechanics testing. Coring in layers above the reservoir is normally accidental

- Many forces act on the formation around the wellbore: mud chemistry, redistribution of stresses, temperature changes etc.

10.1 Strength of rock

An object will fail when the stresses in the material exceed the strength of the rock. There are often micro cracks or fissures in certain direction due to geologic processes, therefore are rocks defined to be heterogeneous. Rocks have also directional properties, and are therefore anisotropic.

10.1.1Tensile strength

Rocks are very weak in tension similarly to metallic materials that have a high tensile strength, σ_t. Most of the rocks contain cracks and therefore its effective tensile strength may approach zero. A common assumption is that the tensile strength is zero. The most common way to determine the tensile strength is with an indirect method called the Brazilian test (Figure 10.1). When loading a circular rock specimen between two plates, the rock becomes elliptical. Then a tensile stress arises in the middle of the rock. At failure the rock will spilt into two or more pieces. Defining the load force as F, the rock diameter as D, and the length as L, the tensile strength is expressed as:

$$\sigma_t = \frac{2F}{\pi DL} \tag{10.1}$$

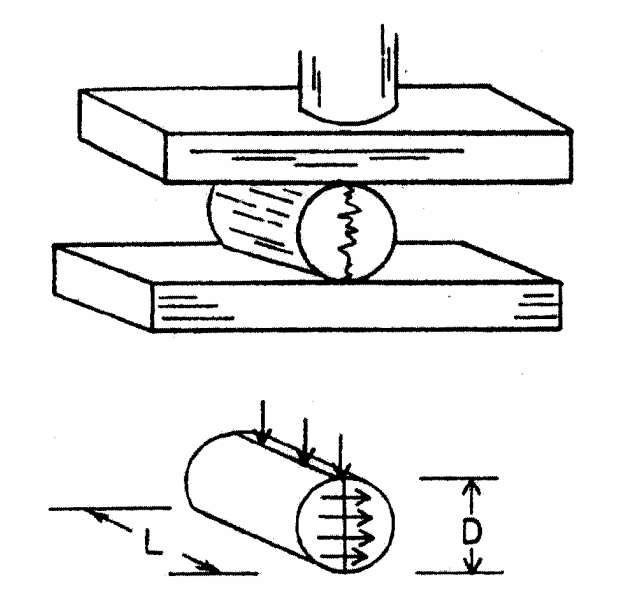

Figure 10.1: Principle for the Brazilian test for tensile strength[3]

10.1.2Shear strength

Shear strength is often called compressional strength. This is because a high compressional loading may result in a shear failure. A rock loaded hydrostatically ($\sigma_x = \sigma_y = \sigma_z$) has a high strength while a rock loaded deviatoric ($\sigma_x \neq \sigma_y \neq \sigma_z$), large shear stress may be the result and failure may take place. Collapse of boreholes is a shear failure. The method to calculate the collapse uses a so called Tri-axial compression cell (Figure 10.2). Core plugs are drilled from cores, covered with an impermeable jacket and then placed in the compression cell.
A predetermined confining pressure is applied, and the plug is loaded axially until it fails.

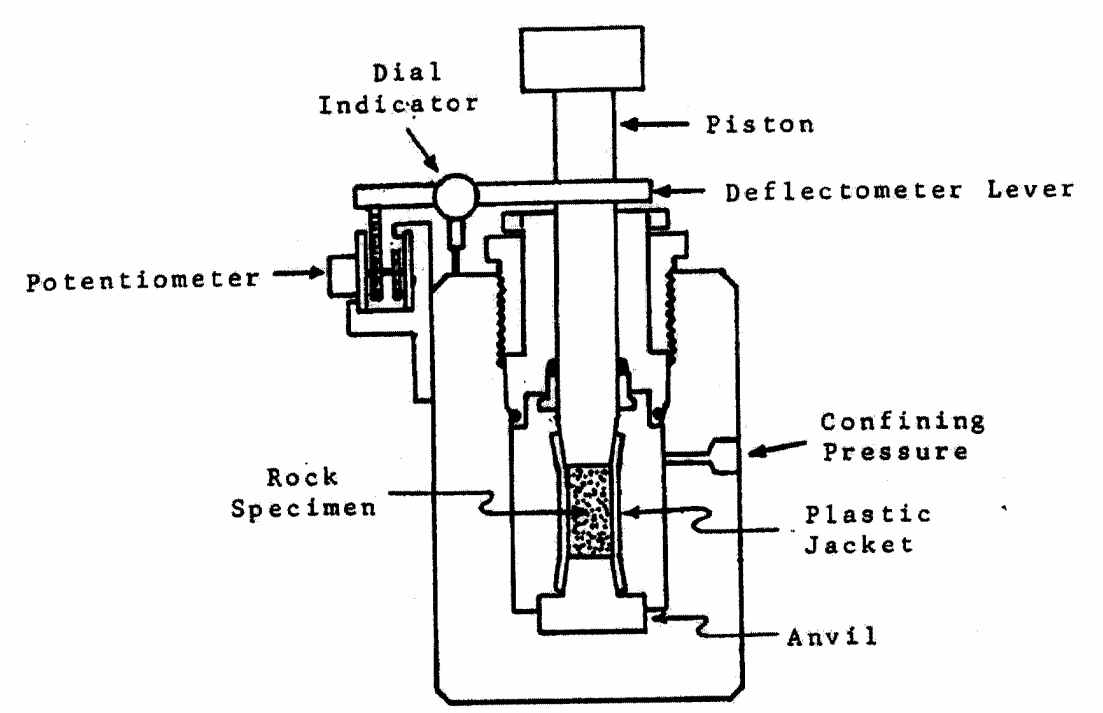

Figure 10.2: Tri-axial compression cell[3]

10.2 General methodology of analysis of borehole stability problems

The object of the analysis is to determine the critical pressure that leads to failure, both fracturing of the borehole and the collapse. Assuming we have the in-situ stresses we must transform these to the direction of the borehole by using the equation 4.3 we found in chapter 4, this equation is also given as equation 10.4 below. Then these are inserted into the Kirsch equations at the borehole wall equation 4.2. We will now have the stresses at the borehole wall. The stresses are inserted into the failure criteria for the borehole to solve for the critical pressures.

We will use effective stress by subtracting the pore pressure. This applies only for normal stresses, not for shear stresses. The failure criteria require principle stresses also.

The principle stresses are found from the stress tensor in equation 10.2[3]

$$[\sigma]=\begin{bmatrix}\sigma_x & \tau_{xy} & \tau_{xz}\\ \tau_{xy} & \sigma_y & \tau_{yz}\\ \tau_{xz} & \tau_{yz} & \sigma_z\end{bmatrix}=\begin{bmatrix}\sigma_1 & 0 & 0\\ 0 & \sigma_2 & 0\\ 0 & 0 & \sigma_3\end{bmatrix} \tag{10.2}$$

When solving equation 10.2 for principal stresses using equation 4.3, the result becomes simplified because two shear stress components vanish. The result becomes:

$$\sigma_r = P_w$$

$$\sigma_2 = \frac{1}{2}(\sigma_\theta + \sigma_Z) + \frac{1}{2}\sqrt{(\sigma_\theta - \sigma_Z)^2 + 4\tau_{\theta Z}^2} \tag{10.3}$$

$$\sigma_3 = \frac{1}{2}(\sigma_\theta + \sigma_Z) - \frac{1}{2}\sqrt{(\sigma_\theta - \sigma_Z)^2 + 4\tau_{\theta Z}^2}$$

After calculation the indexes must be changed such that 1 always refers to the maximum compressive principle stress, 2 to the intermediate and 3 to the least principle stress.

For an inclined well, we have to transform the in-situ stresses to the orientation of the borehole. This is done by using the equation 10.4[3] also know as equation 4.3.

$$\sigma_x = (\sigma_H \cos^2\phi + \sigma_h \sin^2\phi)\cos^2\gamma + \sigma_v \sin^2\gamma$$

$$\sigma_y = (\sigma_H \sin^2\phi + \sigma_h \cos^2\phi)$$

$$\sigma_{zz} = (\sigma_H \cos^2\phi + \sigma_h \sin^2\phi)\sin^2\gamma + \sigma_v \cos^2\gamma \tag{10.4}$$

$$\tau_{yz} = \frac{1}{2}(\sigma_h - \sigma_H)\sin(2\phi)\sin\gamma$$

$$\tau_{xz} = \frac{1}{2}(\sigma_H \cos^2\phi + \sigma_h \sin^2\phi - \sigma_v)\sin(2\gamma)$$

$$\tau_{xy} = \frac{1}{2}(\sigma_h - \sigma_H)\sin(2\phi)\cos\gamma$$

To find the stresses acting on the borehole wall we use the Kirsch equations defined in chapter 4. Further we defined that at the borehole wall r=a, so the equations become:

Radial stress: $\sigma_r = P_w$

Tangential stress: $\sigma_\theta = \sigma_x + \sigma_y - P_w - 2(\sigma_x - \sigma_y)\cos(2\theta) - 4\tau_{xy}\sin(2\theta)$

Axial stress, plane strain: $\sigma_z = \sigma_{zz} - 2\gamma(\sigma_x - \sigma_y)\cos(2\theta) - 4\mu\tau_{xy}\sin(2\theta)$ (10.5)

Axial stress, plane stress: $\sigma_z = \sigma_{zz}$

Shear stress: $\tau_{\theta z} = 2(\tau_{yz}\cos\theta - \tau_{xz}\sin\theta)$

$\tau_{rz} = \tau_{r\theta} = 0$

The results from equation 10.5 are used as input in equation 10.3 to calculate the principal stresses.

10.3 Borehole fracturing

It is important to avoid fracturing during the drilling phase due to the high costs of the drilling mud and inability to "repair" fractures.

The borehole will fracture when the rock stress changes from compression to tension. By increasing the borehole pressure, the hoop stress reduces accordingly. Therefore, fracturing occur at high borehole pressures. The borehole will fracture when the minimum effective principal stress reaches the tensile rock strength σ_t. This is expressed as:

$$\sigma_3^{'} = \sigma_3 - P_0 \le \sigma_t \quad (10.6)$$

Inserting equation 10.3 into equation 10.6, the critical tangential stress becomes:

$$\sigma_\theta = \frac{\tau_{\theta z}^2}{\sigma_z - \sigma_t - P_0} + P_0 + \sigma_t \quad (10.7)$$

Inserting the equation for the tangential stress, equation 10.5, the critical borehole pressure is given by equation 10.8[3]:

$$P_w = \sigma_x + \sigma_y - 2(\sigma_x - \sigma_y)\cos(2\theta) - \frac{\tau_{\theta z}^2}{\sigma_z - \sigma_t - P_0} - P_0 - \sigma_t \quad (10.8)$$

There is another unknown for the general case. The fracture may not arise in the direction of the x or y axis because of shear effects. To resolve this issue, the equation is differentiated to define the extremal conditions. We assume a plane stress case for simplicity, the result becomes:

$$\frac{dP_w}{d\theta} = 0 \rightarrow \tan(2\theta) = 2\frac{\tau_{xy}(\sigma_z - \sigma_t - P_0) - \tau_{xz}\tau_{yz}}{(\sigma_x - \sigma_y)(\sigma_z - \sigma_t - P_0) - \tau_{xz}^2 - \tau_{yz}^2}$$

The normal stresses are in general much larger than the shear stresses. The shear stress components are of second order and are therefore negligible, so the equation is reduced to:

$$\tan(2\theta) = \frac{2\tau_{xy}}{(\sigma_x - \sigma_y)} \qquad (10.9)$$

Equation 10.8 is the general fracturing equation and it is valid for fractures in all directions and for anisotropic stresses.

If symmetric conditions exist, all shear stress components vanish. The fracture will now take place at one of the following conditions: $\sigma_H = \sigma_h, \gamma = 0°, \phi = 0°, 90°$. We can also assume that the rock has zero tensile strength because the rock may contain cracks and fissures. If we assume these conditions, the fracture equations become:

$$P_w = 3\sigma_x - \sigma_y - P_0 - \sigma_t \qquad \text{for } \sigma_x < \sigma_y \text{ , and } \theta = 90° \qquad (10.10a)$$

$$P_w = 3\sigma_y - \sigma_x - P_0 - \sigma_t \qquad \text{for } \sigma_y < \sigma_x \text{ , and } \theta = 0° \qquad (10.10b)$$

These equations say that a fracture will initiate normal to the least stress, and propagate in the direction of the largest normal stress. The equations are strictly valid if the borehole direction is aligned with the in-situ stress direction[3]. If we assume a maximum and minimum normal stress to the borehole wall and the shear stresses have vanished, the general fracture equation becomes:

$$P_w = 3\sigma_{\min} - \sigma_{\max} - P_0 - \sigma_t$$

10.4 Borehole collapse

Borehole collapse is the other main failure mechanism of boreholes. Collapse is a phenomenon associated with low borehole pressures. At low borehole pressures the tangential stress become large. Since there now are a considerable stress contrast between the radial and the tangential stress a considerable shear stress arise. If a critical stress level is exceeded the borehole will collapse in shear.

The maximum principal stress is dominated by the tangential stress, and is given by:

$$\sigma_1 = \frac{1}{2}(\sigma_\theta + \sigma_Z) + \frac{1}{2}\sqrt{(\sigma_\theta - \sigma_Z)^2 + 4\tau_{\theta Z}^2} \tag{10.11}$$

and the minimum principal stress is given by:

$$\sigma_3 = P_w \tag{10.12}$$

If conditions exist that the shear stress vanishes, such as $\sigma_H = \sigma_h, \gamma = 0°, \phi = 0°,$ the maximum principal stress becomes:

$$\sigma_1 = \sigma_\theta \tag{10.13}$$

If we differentiate the maximum principal stress equation we can determine the position on the borehole wall at which the collapse will occur, but this is very complicated. Instead we solve the case where the shear stress vanishes. Inserting equation 10.5 into equation 10.13, we get:

$$\frac{d\sigma_\theta}{d\theta} = 0 \rightarrow \tan(2\theta) = \frac{\tau_{xy}(\sigma_z - P_0) - \tau_{xz}\tau_{yz}}{(\sigma_x - \sigma_y)(\sigma_z - P_0) - \tau_{xz}^2 - \tau_{yz}^2}$$

The normal stresses are in general much larger than the shear stresses. The shear stress components are of second order and are therefore negligible, so the equation is reduced to:

$$\tan(2\theta) = \frac{\tau_{xy}}{(\sigma_x - \sigma_y)} \tag{10.14}$$

The resulting position of the collapse at the borehole is inserted in to the Kirsch equation 10.5, which again are inserted into 10.11, giving the principal stresses at the borehole wall.

If symmetric conditions exist, all shear stress components vanish. The collapse failure may now take place at one of the following conditions: $\sigma_H = \sigma_h, \gamma = 0°, \phi = 0°,90°.$ If we insert this condition into equation 10.5, the borehole pressure causing the highest tangential stress is:

$$\sigma_1 = 3\sigma_y - \sigma_x - P_w \qquad \text{for } \sigma_x < \sigma_y \text{ , and } \theta = 90° \tag{10.15a}$$

$$\sigma_1 = 3\sigma_x - \sigma_y - P_w \qquad \text{for } \sigma_y < \sigma_x \text{ , and } \theta = 0° \tag{10.15b}$$

These equations says that the borehole collapse will initiate in the direction to the least stress.[3] Equation 10.15 is strictly valid if the borehole direction is aligned with the in-situ stress direction. For the general case equation 10.11 will be used.

Now we have the expression for the minimum and maximum principal stresses, a failure criterion is needed to calculate the critical pressure for the general case of borehole collapse. In chapter 5 two different failure criterions where presented.

10.5 Stability in highly inclined boreholes

The conditions in a well will be worse if the well is deviated. This is also true for the stress layers. The vertical stress, which in generally is the largest, will have an increasing component normal to the wellhole as the deviation angle increase, and the stable range for the mudweight decreases.

10.5.1 Borehole fracturing

The fracturing gradient generally decreases with increased borehole inclination. This can also been seen from the curves generated by Aadnøy & Chenevert[4] for a vertical and a horizontal borehole, which are shown in figure 10.3.

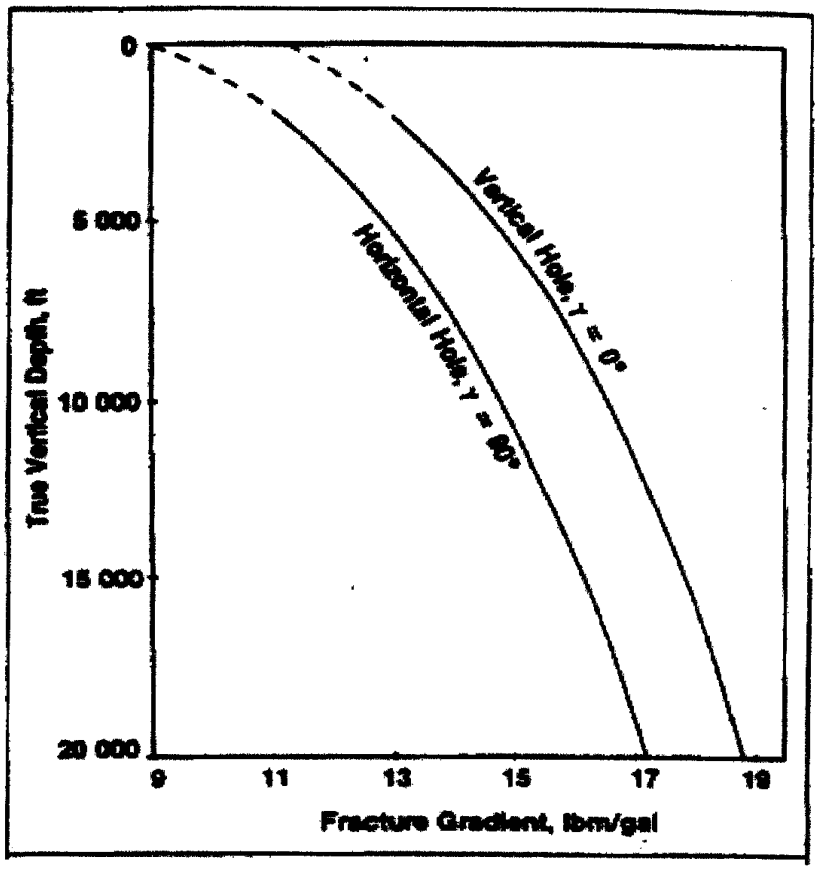

Figure 10.3: Fracture gradient for deviated boreholes[4]

The curves show a significant spread in the fracturing gradients for the two boreholes. So in a normally stress region, an inclined borehole will fracture and lose circulation at a lower borehole pressure than the fracturing pressure of a vertical well.

10.5.2 Borehole collapse

When the wellhole is rotated from a vertical to a horizontal position, the analysis shows that the borehole becomes more sensitive towards collapse. The effect of increasing inclination on the stability of the hole can be seen from figure 10.4. In the figure there are typical failure envelopes for three different rocks are presented. The von Mises Yield criterion is used to generate the diagram.

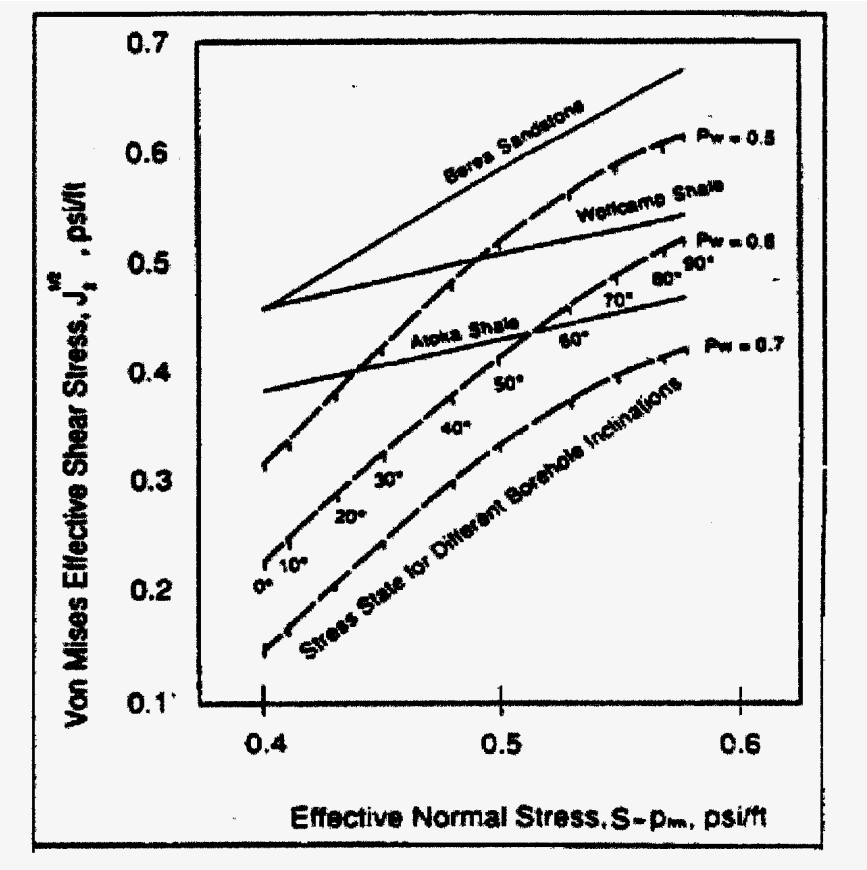

Figure 10.4: von Mises shear failure diagram[4]

From the diagram we can see that an increase of the borehole pressure reduces the stress state away from the failure envelope. So a higher mudweight will keep the borehole stable. If the mudweight gets too high it approaches the fracturing curve and the danger of tensile failure will occur. According to Aadnøy & Chenevert[4] the increase of the in-situ stress field with depth causes the well to become more sensitive towards collapse at greater depths. From studies where Mohr-Coulomb criterion have been used as a basis, it has been concluded that the borehole becomes more susceptible toward collapse the greater the inclination.

11 Modelling of the in-situ stress field on Yme

11.1 Collection of raw data

The limit of data from Yme makes it difficult to predict an accurate borehole stability evaluation. I have all the data I need from 6 wells, while I haven't got the azimuth from 6 wells. The lack of azimuth is because I got LOT from the 6 wells from a borehole stability plot, and it was impossible to say what kind of wells the different LOT's belonged to.
All data used refers to RKB. The raw data is shown in appendix A.

11.1.1Fracturing data

The fracturing data are obtained from well pressure gradients plot. As mentioned above few LOT data exists, while there are several more FIT from the wells.

11.1.2Pore pressure data, P_o

The pore pressures are also obtained from well pressure gradients plot.

11.1.3Overburden data, σ_v

The overburden data are also obtained from well pressure gradients plot.

11.1.4Azimuth, β

Azimuth data are collected from the survey data for each well. Since it's impossible to separate 6 of the wells from the well pressure gradients plot, I couldn't find the azimuth for these 6 wells.

11.1.5Inclination, γ

Inclination data can be collected from the well pressure gradients plot or more accurate from the survey data for each well.

11.2 Modelling of LOT data

First LOT data in sg without any corrections are plotted against depth. This is shown in figure 11.1.

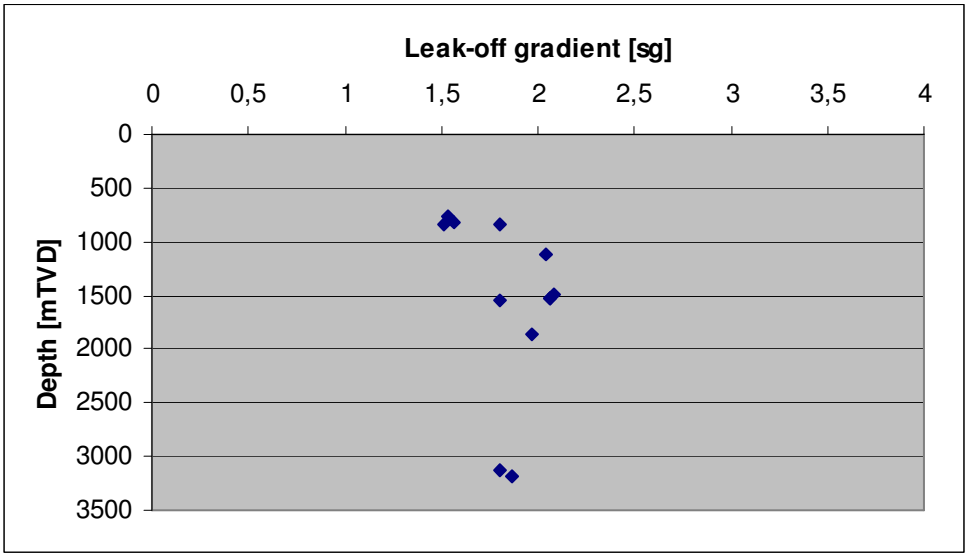

Figure 11.1: Raw data LOT in sg

The LOT data shows an increase with depth, this is expected. The LOT does not fall on a straight line, and a best-fit curve needs to be estimated. Converting the LOT data to pressure, a better correlation is obtained. The conversion is done by using equation 11.1.

$$P = \rho \cdot 0{,}098 \cdot D_{TVD} \qquad (11.1)$$

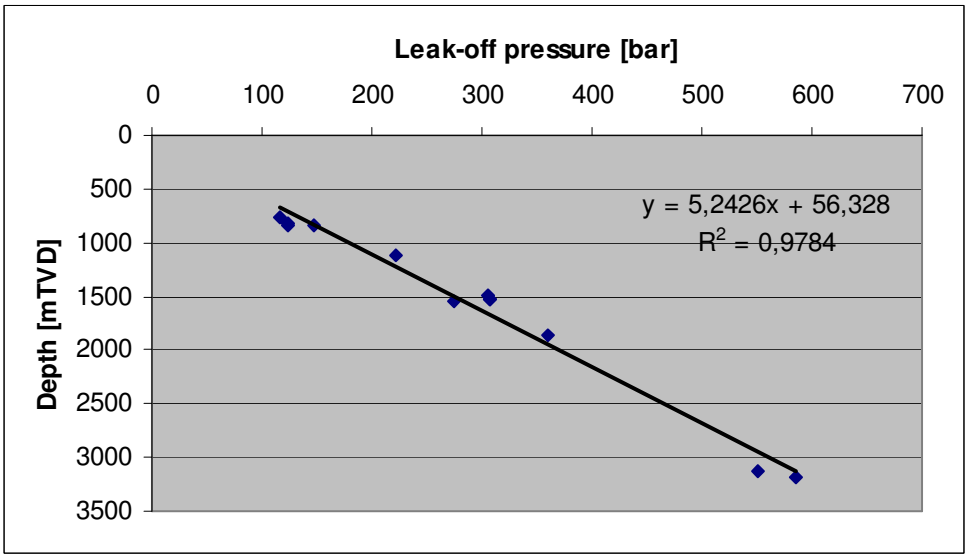

Figure 11.2: Raw data LOT in bar

The next step is to normalize for the different borehole inclination. This is done by using equation 7.5:

$$P_{wf}(0) = P_{wf}(\gamma) + \frac{\left(\sigma_v - \frac{1}{2}P_o\right)\sin^2\gamma}{1 + \frac{1}{2}\sin^2\gamma} \qquad (11.2)$$

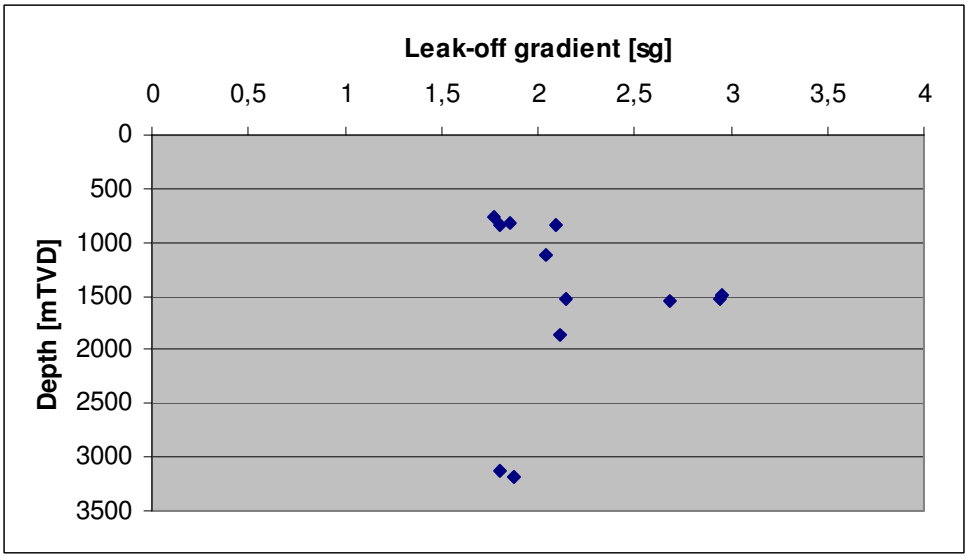

Figure 11.3: LOT corrected to vertical in sg

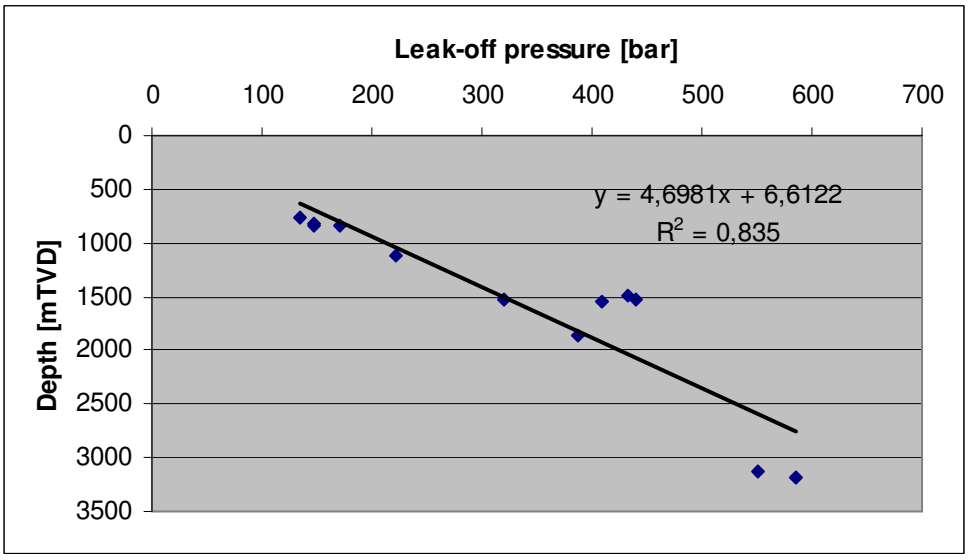

Figure 11.4: LOT corrected to vertical in bar

A trend line from the pressure plot was generated from the last square method. And expression for the LOT pressure as a function of depth will then be:

$$D_{TVD} = \alpha \cdot P_{LOT} + \beta \qquad (11.3)$$

Where α is the slope and β is the intercept. The resulting equation for the trendline in figure 11.4 will then be:

$$D_{TVD} = 4{,}6981 \cdot P_{LOT} + 6{,}6122 \qquad (11.4)$$

The LOT value for any depth can be found from equation 11.4. To find the best-fit curve in any gradient plot, equation 11.3 for the straight line is inserted in to the general gradient equation 11.1, which gives equation 11.5:

$$P_{wf,sg}(0°) = \frac{D_{TVD} - \beta}{\alpha \cdot 0{,}098 \cdot D_{TVD}} \qquad (11.5)$$

For figure 11.1, a trendline with α = 5,2426 and β = 56,328 inserted in equation 11.5 can be found. And for figure 11.3 with α = 4,6981 and β = 6,6122.

In figure 11.3 and 11.4, the LOT for 3 of the points becomes higher compared to the other LOT. The reason for this is not known.

From the pore pressure data seen in appendix A, we can seen that using the compaction model for normalizing the LOT to the same pore pressure will not give us much more improved data. And with a conversation with Bernt S. Aadnøy it was decided to drop the compaction model.

11.3 Inversion technique

In the Inversion technique only 6 data sets are used. This is as mentioned earlier the lack of azimuth for 6 of the data sets.

Data Set	Well	Casing	Depth mTVD RKB	Po,sg	Pwf,sg	Ob,sg	Inc	Az
1	_9/2-9S	13 3/8"	1867	1,03	1,97	2,04	19,07	282
2	_9/2-A-8	13 3/8"	1520	1	2,06	1,94	14,29	41,73
3	_9/2-A-4	20"	832	0,98	1,56	1,74	30,95	6,88
4	_9/2-3	20"	1110	1,03	2,04	1,85	0,9	253,4
5	"	9 5/8"	3190	1,27	1,87	2,19	1,87	250,3
6	_9/2-5	9 5/8"	3120	1,23	1,8	2,18	0,72	220,3

Table11.1: Input data for the inversion technique

First all the data sets are used in the simulation. This is to estimate an average stress in the formation. The simulation gave the following result:

$\sigma_H/\sigma_v = 0.783$

$\sigma_h/\sigma_v = 0.758$

$\beta = 119$

$e^2 = 0{,}045$

Data set	1	2	3	4	5	6
Meas. LOT	1,97	2,06	1,56	2,04	1,87	1,8
Predicted LOT	2,01	1,88	1,54	1,82	2,09	2,03

Table 11.2: LOT data from the simulation

The interpretation of the result is as follow:

The maximum principal horizontal stress is 0.783 times the overburden stress, and its direction is 119 degrees from North. The minimum principal stress is 0.758 times the overburden stress. These results are in the region for what looks like a trend for the North Sea. The data covers a considerable depth interval and a large geographical area. Therefore simulations under/around each casing shoe will be done. From the table 11.2 the predicted LOT of each data set is shown. If the measured and the predicted data are similar, the model is good. Comparison between the measured and the predicted leak-off data shows a poor correlation. For practical application, this difference should probably be within 0.05 – 0.10 $s.g^3$. So except for data set 1 and 3 the model is not adequate for this field. And the field has to be model with several sub models. In this case, one model for each casing shoe.

Location: Casing shoe 20":

In this case data set 3 and 4 are used, which is in 832 - 1110m depth.
The simulation gave the following results:

$\sigma_H/\sigma_v = 1.030$

$\sigma_h/\sigma_v = 0.823$

$\beta = 104$

$e^2 = 0$

Data set	3	4
Meas. LOT	1,56	2,04
Predicted LOT	1,56	2,04

Table 11.3: LOT from data set 3 and 4

The largest principal horizontal stress is 1.030 times the overburden stress, and its direction is 104 degrees from North. The minimum principal stress is 0.823 times the overburden stress. The maximum and the minimum principal stress give a poor comparison. This gives a good indication of an anisotropy stress field. The quality of the simulation shows a perfect match and a correct assessment of the stress state at this depth level is considered.

Location: Casing shoe 13 3/8":

In this case data set 1 and 2 are used, which is in 1520 – 1867m depth.

The simulation gave the following results:

$\sigma_H/\sigma_v = 0.803$

$\sigma_h/\sigma_v = 0.774$

$\beta = 4$

$e^2 = 0$

Data set	1	2
Meas. LOT	1,97	2,06
Predicted LOT	1,97	2,06

Table 11.4: LOT from data set 1 and 2

The largest principal horizontal stress is 0.803 times the overburden stress, and its direction is 4 degrees from North. The minimum principal stress is 0.774 times the overburden stress. The maximum and the minimum principal stress give an okay comparison. But this gives also an indication of an anisotropy stress field. The quality of the simulation shows a perfect match and a correct assessment of the stress state at this depth level is considered.

Location: Casing shoe 9 5/8":

In this case data set 5 and 6 where used which is in 3120-3190m depth.

$\beta = 55$

Data set	5	6
Meas LOT	1,87	1,8
Predicted LOT	1,95	1,82

Table 11.5: LOT from data set 5 and 6

The relative magnitude of the maximum and minimum principal stress to the overburden became extreme large, and could not be used. So manual calculation where done.
Equation 9.3a where used:

$$\frac{P_{wf} + P_o}{\sigma_v} + \sin^2\gamma = \left(3\sin^2\phi - \cos^2\phi\cos^2\gamma\right)\frac{\sigma_k}{\sigma_v} + \left(3\cos^2\phi - \sin^2\phi\cos^2\gamma\right)\frac{\sigma_l}{\sigma_v} \quad (11.6)$$

The equation gave the following result:

$\sigma_H = 1{,}56$

$\sigma_h = 1{,}49$

The direction is 55 degrees from North.

12 Fracture and Collapse calculation

In this chapter fracturing and collapse pressure for the 5 wells will presented. The calculation uses the in-situ stresses from the inversion technique as input together with the inclination and azimuth of the wells. Overburden and pore pressures from the formation are also used.

12.1 Input data

Cohesion strength, τ_0:

The cohesion strength τ_0 was decided to put equal to a constant value of 0,2sg.

Angle of internal friction, α:

The angle of internal friction α was decided to put equal to a constant value of 30°.

Maximum horizontal stress, σ_H:

The maximum horizontal stress is taken from the inversion technique. By multiplying the relative magnitudes (σ_H/σ_v) with the overburden stress for each depth, the maximum horizontal stress is found.

Minimum horizontal stress, σ_h:

The minimum horizontal stress is found the same way as the maximum horizontal stress.

12.2 Manual fracturing and collapse calculations

12.2.1 Fracturing

First the in-situ stresses are transformed into the orientation of the borehole. This is done by using the equation 4.3. Secondly the stresses at the borehole wall have to de decided. This is done by equation 4.2. These results are inserted into equation 10.8:

$$P_w = \sigma_x + \sigma_y - 2(\sigma_x - \sigma_y)\cos(2\theta) - \frac{\tau_{\theta z}^2}{\sigma_z - \sigma_t - P_0} - P_0 - \sigma_t \qquad (12.1)$$

The tensile strength σ_t is set equal to zero. The position of the fracture on the borehole wall θ, is found by equation 10.9:

$$\tan(2\theta) = \frac{2\tau_{xy}}{(\sigma_x - \sigma_y)} \qquad (12.2)$$

12.2.1 Collapse

The Mohr-Coulomb shear model given by equation 5.7, where used as the failure criterion for calculating the collapse.

$$\frac{1}{2}(\sigma'_1-\sigma'_3)\cos\phi=\tau_0+\left[\frac{1}{2}(\sigma'_1+\sigma'_3)-\frac{1}{2}(\sigma'_1-\sigma'_3)\sin\phi\right]\tan\phi \qquad (12.3)$$

The maximum effective principal stress is given by equation 10.11:

$$\sigma_1^{'}=\frac{1}{2}(\sigma_\theta+\sigma_Z)+\frac{1}{2}\sqrt{(\sigma_\theta-\sigma_Z)^2+4\tau_{\theta Z}^2}-Po \qquad (12.4)$$

The minimum effective principal stress is given by equation 10.12:

$$\sigma_3^{'}=P_w-Po \qquad (12.5)$$

12.2.3 Result

In the following the fracturing and collapse gradients are shown for each well. In appendix B all results are shown for each well. And in appendix C the full calculation for well 9/2-9S at 1867m is shown as an example.

9/2-9S				
mTVD	σH [sg]	σh[sg]	Pwf[sg]	Pwc[sg]
950	1,88	1,51	3,06	1,36
1867	1,64	1,58	2,26	1,17
3122	1,56	1,49	1,42	1,11

Table 12.1: Fracture and collapse gradients for well 9/2-9S

9/2-A-8				
mTVD	σH [sg]	σh[sg]	Pwf[sg]	Pwc[sg]
830	1,8	1,46	1,33	1,01
1520	1,56	1,5	1,94	1,07
3130	1,56	1,49	1,17	1,01

Table 12.2: Fracture and collapse gradients for well 9/2-A-8

9/2-A-4				
mTVD	σH [sg]	σh[sg]	Pwf[sg]	Pwc[sg]
832	1,79	1,43	1,53	0,94
1600	1,574	1,517	1,7	1
3130	1,56	1,49	1,73	1,15

Table 12.3: Fracture and collapse gradients for well 9/2-A-4

9/2-3				
mTVD	σH [sg]	σh[sg]	Pwf[sg]	Pwc[sg]
1110	1,9	1,52	3,15	1,3
1825	1,64	1,58	2,31	1,176
3190	1,56	1,49	1,91	1,26

Table 12.4: Fracture and collapse gradients for well 9/2-3

9/2-5				
mTVD	σH [sg]	σh[sg]	Pwf[sg]	Pwc[sg]
960	1,895	1,514	1,62	1,01
1760	1,638	1,579	2,07	1,12
3120	1,56	1,49	1,68	1,17

Table 12.5: Fracture and collapse gradients for well 9/2-5

A fracturing gradient over 2.0sg is unrealistic, and from the tables above several of the fracturing gradients are over 2.0sg. And in well 9/2 A-8 some of the fracturing gradients are too low. The reason for the high fracturing gradients for some of the wells and the low fracturing gradients for well 9/2 A-8, may be caused by data inconsistency from collection of the data from many different sources. Also a geological uncertainty related to the faults and tectonic forces present represents a factor.

Some of the collapse gradients above are lower than the pore pressure gradients for the wells. In reality an inward flow would occur as, for example, during underbalanced drilling.
The calculation method above is valid only when the collapse pressure is higher than the pore pressure[3].

By comparing the fracturing and collapse gradients for the different wells it is seen that wells 9/2-9S and 9/2-3 have an overall higher fracturing gradient compared to the other wells. The azimuth seems to be the reason for this, since both this wells have a large azimuth compared to the other wells.

13 Summary

In this thesis the Inversion technique are used to perform an analysis of the in-situ stresses around Yme. The results of the analysis where used together with data form each well to calculate fracture and collapse gradients for the wells.

- The limit of data from Yme made it difficult to predict an accurate borehole stability evaluation

- The in-situ stress field is found to be anisotropic.

- Azimuth is proven to have a large effect on the fracturing gradient and a smaller effect on the collapse gradient

- The fracturing gradient became unrealistic large for several of the wells, and too low for some gradients in well 9/2 A-8. The cause may be data inconsistency from collection of the data from many different sources. Also a geological uncertainty related to the faults and tectonic forces present represents a factor.

Reference

(1) Røland B, (2006), Plan for development and operation, internal document Talisman Energy.

(2) Aadnøy B.S, (1999), Modern well design

(3) Aadnøy B.S, (1997, rev 2003), An introduction to petroleum rock mechanics, compendium, University of Stavanger

(4) Aadnøy B.S. and Chenevert M.E, (1987), Stability of highly inclined boreholes, SPE 16052, Drilling Engineering

(5) Hansen A.K, (2002), Analysis of Borehole Stability on Snorre TLP, Master thesis, University of Stavanger

(6) http://www.glossary.oilfield.slb.com/Display.cfm?Term=leakoff%20test

(7) Fjær E, Holt R.M, Horsrud P, Raaen A.M and Risnes R, (1992), Petroleum related rock mechanics.

Table of figures

Nomenclature

BE	Beta East
BNW	Beta North West
BSW	Beta South West
GW	Gamma West
GNE	Gamma North West
GSE	Gamma South East
ELOT	Extended leak-off test
LOT	Leak-off test
FIT	Formation integrity test
RF	Recovery factor
SWAG	Simultaneous water and gas
MMstb	Million Stock Tank Barrels
Sm^3	Standard cubic meter
STOIIP	Stock Tank Oil Initially in Place
SG	Specific gravity
TVD	True vertical depth
RKB	drill floor depth reference point

F	Force
FN	Force acting normal to a plane
FS	Force acting parallel to a plane
Po	Pore pressure
Pwf	Fracturing pressure
Pwc	Collapse pressure
PLOT	Leak-off pressure [bar]
θ	Angle relative to the x-axis
σ	Normal stress
τ	Shear stress
σ_r	Radial stress
σ_z	Axial stress

σ_θ	Tangential stress
σ_m	Average stress
σ_v	Overburden stress, vertical stress
σ_H	Maximum horizontal principal in-situ stress
σ_h	Minimum horizontal principal n-situ stres
σ_t	Tensile strength
ν	Poisson's ratio
E	Young's modulus
a	Radius of the hole
r	Position radially outwards from center
ρ	Pressure gradient [sg]
e	error
ø	Azimuth of the well
γ	Inclination of the well
α	Angle of internal friction
β	Angle of failure
τo	Cohesion
I	Invariant
J2	Second deviatoric invariant
DTVD	Depth in mTVD RKB

Appendix A

Well	Casing	Depth mTVD RKB	Po,sg	Pwf,sg	Ob,sg	Inc	Az
_9/2-9S	13 3/8"	1867	1,03	1,97	2,04	19,07	282
_9/2-A-8	13 3/8"	1520	1	2,06	1,94	14,29	41,73
_9/2-A-4	20"	832	0,98	1,56	1,74	30,95	6,88
_9/2-8S, t2,t3,t4	20"	770	0,97	1,53	1,72	28	N/A
"	20"	831	0,98	1,51	1,76	30,5	N/A
"	20"	831	0,98	1,8	1,76	30,5	N/A
"	13 3/8"	1551	1	1,8	1,95	70	N/A
"	13 3/8"	1525	1	2,06	1,94	70	N/A
"	13 3/8"	1495	1	2,08	1,93	70	N/A
_9/2-3	20"	1110	1,03	2,04	1,85	0,9	253,4
"	9 5/8"	3190	1,27	1,87	2,19	1,87	250,3
_9/2-5	9 5/8"	3120	1,23	1,8	2,18	0,72	220,3

Appendix B

9/2-9S

mTVD = 950m
Po = 1,03
$O_{b\,sg}$ = 1,83
Inc = 20,32
Azi = 281,7

σ_H = 1,88
σ_h = 1,51

Calculation of fracture:

$\sigma_x = 1{,}56$
$\sigma_y = 1{,}862$
$\sigma_{zz} = 1{,}793$
$\tau_{yz} = -0{,}026$
$\tau_{xz} = -0{,}099$
$\tau_{xy} = 0{,}0689$

$\theta = -12{,}26°$

$\sigma_r = Pw$
$\sigma_\theta = 4{,}086 - Pw$
$\sigma_z = 1{,}793$
$\tau_{\theta z} = 0{,}0088$

$P_{wf} = 3{,}06sg$

Calculation of collapse:

$\theta = -6{,}43°$

$\sigma_r = Pw$
$\sigma_\theta = 4{,}074 - Pw$
$\sigma_z = 1{,}793$
$\tau_{\theta z} = 0{,}0295$

$\sigma_1 = 4{,}07 - Pw$

$\sigma_1^{'} = 3{,}04 - Pw$

$\sigma_3 = Pw$

$\sigma_3^{'} = Pw - 1{,}03$

$P_{wc} = 1{,}36sg$

mTVD = 1867m
Po = 1,03
$O_{b\ sg}$ = 2,04
Inc = 19,07
Azi = 282

σ_H = 1,64
σ_h = 1,58

Calculation of fracture:

$\sigma_x = 1{,}63$

$\sigma_y = 1{,}637$

$\sigma_{zz} = 1{,}991$

$\tau_{yz} = 0{,}00399$

$\tau_{xz} = -0{,}14$

$\tau_{xy} = 0{,}011$

$\theta = -36{,}54°$

$\sigma_r = Pw$

$\sigma_\theta = 3{,}3131 - Pw$

$\sigma_z = 1{,}991$

$\tau_{\theta z} = -0{,}159$

$P_{wf} = 2{,}26sg$

Calculation of collapse:

$\theta = -29{,}34°$

$\sigma_r = Pw$
$\sigma_\theta = 3{,}3123 - Pw$
$\sigma_z = 1{,}991$
$\tau_{\theta z} = -0{,}13$

$\sigma_1 = 3{,}325 - Pw$
$\sigma_1^{'} = 2{,}295 - Pw$

$\sigma_3 = Pw$
$\sigma_3^{'} = Pw - 1{,}03$

$P_{wc} = 1{,}17\,sg$

mTVD = 3120m
Po = 1,23
$O_{b\,sg}$ = 2,18
Inc = 51,27
Azi = 314,27

σ_H = 1,56
σ_h = 1,49

Calculation of fracture:

$\sigma_x = 1{,}92$
$\sigma_y = 1{,}53$
$\sigma_{zz} = 1{,}78$
$\tau_{yz} = 0{,}0273$
$\tau_{xz} = -0{,}32$
$\tau_{xy} = 0{,}0219$

$\theta = 3{,}2°$

$\sigma_r = Pw$
$\sigma_\theta = 2{,}665 - Pw$
$\sigma_z = 1{,}78$
$\tau_{\theta z} = 0{,}09$

$P_{wf} = 1{,}42sg$

Calculation of collapse:

$\theta = 1{,}6°$

$\sigma_r = Pw$
$\sigma_\theta = 2{,}67 - Pw$
$\sigma_z = 1{,}78$
$\tau_{\theta z} = 0{,}07238$

$\sigma_1 = 2{,}681 - Pw$
$\sigma_1^{'} = 1{,}451 - Pw$

$\sigma_3 = Pw$
$\sigma_3^{'} = Pw - 1{,}23$

$P_{wc} = 1{,}11sg$

9/2-A-8

mTVD = 830m
Po = 0,98
$O_{b\ sg}$ = 1,75
Inc = 14,92
Azi = 39,79

σ_H = 1,8
σ_h = 1,46

Calculation of fracture:

$\sigma_x = 1{,}665$
$\sigma_y = 1{,}6$
$\sigma_{zz} = 1{,}744$
$\tau_{yz} = -0{,}043$
$\tau_{xz} = -0{,}32$
$\tau_{xy} = -0{,}162$

$\theta = -39{,}3°$

$\sigma_r = Pw$
$\sigma_\theta = 2{,}6 - Pw$
$\sigma_z = 1{,}744$
$\tau_{\theta z} = -0{,}472$

$P_{wf} = 1{,}33sg$

Calculation of collapse:

$\theta = -34{,}07°$

$\sigma_r = Pw$
$\sigma_\theta = 2{,}62 - Pw$
$\sigma_z = 1{,}744$
$\tau_{\theta z} = -0{,}43$

$\sigma_1 = 2{,}794 - Pw$
$\sigma_1^{'} = 1{,}814 - Pw$

$\sigma_3 = Pw$

$\sigma_3^{'} = Pw - 0{,}98$

$P_{wc} = 1{,}01sg$

mTVD = 1520m
Po = 1
$P_{w,sg}$ = 2,06
$O_{b\,sg}$ = 1,94
Inc = 14,29
Azi = 41,73

σ_H = 1,56
σ_h = 1,50

Calculation of fracture:

$\sigma_x = 1{,}558$

$\sigma_y = 1{,}526$

$\sigma_{zz} = 1{,}915$

$\tau_{yz} = -0{,}074$

$\tau_{xz} = -0{,}097$

$\tau_{xy} = -0{,}029$

$\theta = -30{,}56°$

$\sigma_r = Pw$

$\sigma_\theta = 2{,}9514 - Pw$

$\sigma_z = 1{,}915$

$\tau_{\theta z} = -0{,}112$

$P_{wf} = 1{,}937sg$

Calculation of collapse:

$\theta = -21{,}1°$

$\sigma_r = Pw$

$\sigma_\theta = 2{,}959 - Pw$

$\sigma_z = 1{,}915$

$\tau_{\theta z} = -0{,}0846$

$\sigma_1 = 2{,}958 - Pw$

$\sigma_1^{'} = 1{,}958 - Pw$

$\sigma_3 = Pw$

$\sigma_3^{'} = Pw - 1$

$P_{wc} = 1{,}07 sg$

---

mTVD = 3130m
Po = 1,19
$O_{b\ sg}$ = 2,16
Inc = 73,75
Azi = 358,4

σ_H = 1,56
σ_h = 1,49

Calculation of fracture:

$\sigma_x = 2{,}11$

$\sigma_y = 1{,}49$

$\sigma_{zz} = 1{,}606$

$\tau_{yz} = 0{,}0019$

$\tau_{xz} = -0{,}1614$

$\tau_{xy} = -0{,}000547$

$\theta = -0{,}05°$

$\sigma_r = Pw$

$\sigma_\theta = 2{,}36 - Pw$

$\sigma_z = 1606$

$\tau_{\theta z} = 0{,}0041$

$P_{wf} = 1{,}17 sg$

Calculation of collapse:

$$\theta = -0{,}025°$$

$$\sigma_r = Pw$$
$$\sigma_\theta = 2{,}36 - Pw$$
$$\sigma_z = 1{,}606$$
$$\tau_{\theta z} = 0{,}0041$$

$$\sigma_1 = 2{,}36 - Pw$$
$$\sigma_1^{'} = 1{,}17 - Pw$$

$$\sigma_3 = Pw$$
$$\sigma_3^{'} = Pw - 1{,}19$$

$$P_{wc} = 1{,}01sg$$

9/2-A-4

mTVD = 832m
Po = 0,98
$P_{w,sg}$ = 1,56
$O_{b\ sg}$ = 1,74
Inc = 30,95
Azi = 6,88

σ_H = 1,79
σ_h = 1,43

Calculation of fracture:

$\sigma_x = 1{,}777$
$\sigma_y = 1{,}435$
$\sigma_{zz} = 1{,}754$
$\tau_{yz} = -0{,}022$
$\tau_{xz} = 0{,}0216$
$\tau_{xy} = -0{,}0367$

$\theta = -6{,}06°$

$\sigma_r = Pw$
$\sigma_\theta = 2{,}32 - Pw$
$\sigma_z = 1{,}754$
$\tau_{\theta z} = -0{,}0394$

$P_{wf} = 1{,}524 sg$

Calculation of collapse:

$\theta = -3{,}06°$

$\sigma_r = Pw$
$\sigma_\theta = 2{,}509 - Pw$
$\sigma_z = 1{,}754$
$\tau_{\theta z} = -0{,}0557$

$\sigma_1 = 2{,}51 - Pw$
$\sigma_1^{'} = 1{,}53 - Pw$

$\sigma_3 = Pw$

$\sigma_3^{'} = Pw - 0{,}98$

$P_{wc} = 0{,}94sg$

mTVD = 1600m
Po = 1
$O_{b\,sg}$ = 1,96
Inc = 58,92
Azi = 3,71

σ_H = 1,574
σ_h = 1,517

Calculation of fracture:

$\sigma_x = 1{,}86$

$\sigma_y = 1{,}52$

$\sigma_{zz} = 1{,}675$

$\tau_{yz} = -0{,}00127$

$\tau_{xz} = -0{,}171$

$\tau_{xy} = -0{,}0019$

$\theta = -0{,}32°$

$\sigma_r = Pw$

$\sigma_\theta = 2{,}7 - Pw$

$\sigma_z = 1{,}675$

$\tau_{\theta z} = -0{,}0045$

$P_{wf} = 1{,}7sg$

Calculation of collapse:

$\theta = -0{,}16°$

$\sigma_r = Pw$
$\sigma_\theta = 2{,}7 - Pw$
$\sigma_z = 1{,}675$
$\tau_{\theta z} = -0{,}0065$

$\sigma_1 = 2{,}7 - Pw$
$\sigma_1^{'} = 1{,}7 - Pw$

$\sigma_3 = Pw$
$\sigma_3^{'} = Pw - 1$

$P_{wc} = 1{,}0sg$

mTVD = 3130
Po = 1,18
$O_{b\ sg}$ = 2,16
Inc = 2,26
Azi = 14,38

σ_H = 1,56
σ_h = 1,49

Calculation of fracture:

$\sigma_x = 1{,}553$
$\sigma_y = 1{,}494$
$\sigma_{zz} = 2{,}159$
$\tau_{yz} = -0{,}00066$
$\tau_{xz} = -0{,}024$
$\tau_{xy} = -0{,}0168$

$\theta = -14{,}38°$

$\sigma_r = Pw$
$\sigma_\theta = 2{,}914 - Pw$
$\sigma_z = 2{,}159$
$\tau_{\theta z} = -0{,}016$

$P_{wf} = 1{,}73 sg$

Calculation of collapse:

$\theta = -7{,}95°$

$\sigma_r = Pw$
$\sigma_\theta = 2{,}917 - Pw$
$\sigma_z = 2{,}159$
$\tau_{\theta z} = -0{,}0093$

$\sigma_1 = 2{,}917 - Pw$
$\sigma_1^{'} = 1{,}737 - Pw$

$\sigma_3 = Pw$
$\sigma_3^{'} = Pw - 1{,}18$

$P_{wc} = 1{,}146 sg$

9/2-3

mTVD = 1110m
Po = 1,03
$P_{w,sg}$ = 2,04
$O_{b\ sg}$ = 1,85
Inc = 0,9
Azi = 253,4

σ_H = 1,9
σ_h = 1,52

Calculation of fracture:

$\sigma_x = 1{,}551$
$\sigma_y = 1{,}869$
$\sigma_{zz} = 1{,}849$
$\tau_{yz} = -0{,}0016$
$\tau_{xz} = -0{,}0049$
$\tau_{xy} = -0{,}104$

$\theta = 16{,}58°$

$\sigma_r = Pw$
$\sigma_\theta = 4{,}179 - Pw$
$\sigma_z = 1{,}849$
$\tau_{\theta z} = -0{,}00038$

$P_{wf} = 3{,}15sg$

Calculation of collapse:

$\theta = 9{,}05°$

$\sigma_r = Pw$
$\sigma_\theta = 4{,}153 - Pw$
$\sigma_z = 1{,}849$
$\tau_{\theta z} = -0{,}00168$

$\sigma_1 = 4{,}153 - Pw$
$\sigma_1' = 3{,}123 - Pw$

$\sigma_3 = Pw$

$\sigma_3^{'} = Pw - 1{,}03$

$P_{wc} = 1{,}38sg$

mTVD = 1825m
Po = 1,03
$O_{b\,sg}$ = 2,04
Inc = 1,33
Azi = 229,14

σ_H = 1,64
σ_h = 1,58

Calculation of fracture:

$\sigma_x = 1{,}605$

$\sigma_y = 1{,}614$

$\sigma_{zz} = 2{,}04$

$\tau_{yz} = -0{,}00069$

$\tau_{xz} = -0{,}01$

$\tau_{xy} = -0{,}0297$

$\theta = 40{,}7°$

$\sigma_r = Pw$

$\sigma_\theta = 3{,}339 - Pw$

$\sigma_z = 2{,}04$

$\tau_{\theta z} = 0{,}012$

$P_{wf} = 2{,}31sg$

Calculation of collapse:

$\theta = 36{,}49°$

$\sigma_r = Pw$

$\sigma_\theta = 3{,}338 - Pw$

$\sigma_z = 2{,}04$

$\tau_{\theta z} = 0{,}011$

$\sigma_1 = 3{,}338 - Pw$

$\sigma_1^{'} = 2{,}308 - Pw$

$\sigma_3 = Pw$

$\sigma_3^{'} = Pw - 1{,}03$

$P_{wc} = 1{,}176 sg$

mTVD = 3190m
Po = 1,27
$P_{w,sg}$ = 1,87
$O_{b\ sg}$ = 2,19
Inc = 1,87
Azi = 250,3

σ_H = 1,56
σ_h = 1,49

Calculation of fracture:

$\sigma_x = 1{,}5$

$\sigma_y = 1{,}55$

$\sigma_{zz} = 2189$

$\tau_{yz} = -0{,}0007$

$\tau_{xz} = -0{,}023$

$\tau_{xy} = -0{,}0722$

$\theta = 20{,}67°$

$\sigma_r = Pw$

$\sigma_\theta = 3{,}183 - Pw$

$\sigma_z = 2{,}189$

$\tau_{\theta z} = -0{,}0149$

$P_{wf} = 1{,}91 sg$

Calculation of collapse:

$\theta = 11.87°$

$\sigma_r = Pw$
$\sigma_\theta = 3{,}177 - Pw$
$\sigma_z = 2{,}189$
$\tau_{\theta z} = 0{,}008$

$\sigma_1 = 3{,}175 - Pw$
$\sigma_1^{'} = 1{,}905 - Pw$

$\sigma_3 = Pw$
$\sigma_3^{'} = Pw - 1{,}27$

$P_{wc} = 1{,}26sg$

9/2-5

mTVD = 960m
Po = 1,03
$O_{b\ sg}$ = 1,84
Inc = 0,4
Azi = 16

σ_H = 1,895
σ_h = 1,514

Calculation of fracture:

$\sigma_x = 1{,}866$
$\sigma_y = 1{,}543$
$\sigma_{zz} = 1{,}84$
$\tau_{yz} = -0{,}0007$
$\tau_{xz} = -0{,}00018$
$\tau_{xy} = -0{,}1$

$\theta = -15{,}9°$

$\sigma_r = Pw$
$\sigma_\theta = 2{,}65 - Pw$
$\sigma_z = 1{,}84$
$\tau_{\theta z} = -0{,}00125$

$P_{wf} = 1{,}62sg$

Calculation of collapse:

$\theta = -8{,}6°$

$\sigma_r = Pw$
$\sigma_\theta = 2{,}674 - Pw$
$\sigma_z = 1{,}84$
$\tau_{\theta z} = -0{,}00133$

$\sigma_1 = 2{,}674 - Pw$
$\sigma_1^{'} = 1{,}644 - Pw$

$\sigma_3 = Pw$
$\sigma_3^{'} = Pw - 1{,}03$

$P_{wc} = 1{,}01sg$

mTVD = 1760m
Po = 1,03
$O_{b\ sg}$ = 2,04
Inc = 1,1
Azi = 194,8

σ_H = 1,638
σ_h = 1,579

Calculation of fracture:

$\sigma_x = 1{,}634$
$\sigma_y = 1{,}583$
$\sigma_{zz} = 2{,}04$
$\tau_{yz} = -0{,}00028$
$\tau_{xz} = -0{,}0078$
$\tau_{xy} = -0{,}0146$

$\theta = -14{,}9°$

$\sigma_r = Pw$
$\sigma_\theta = 3{,}1 - Pw$
$\sigma_z = 2{,}04$
$\tau_{\theta z} = -0{,}0046$

$P_{wf} = 2{,}07 sg$

Calculation of collapse:

$\theta = -7{,}3°$

$\sigma_r = Pw$
$\sigma_\theta = 3{,}104 - Pw$
$\sigma_z = 2{,}04$
$\tau_{\theta z} = -0{,}0025$

$\sigma_1 = 3{,}1 - Pw$
$\sigma_1' = 2{,}07 - Pw$

$\sigma_3 = Pw$
$\sigma_3' = Pw - 1{,}03$

$P_{wc} = 1{,}12 sg$

mTVD = 3120m

Po = 1,23
$P_{w,sg}$ = 1,8
$O_{b\,sg}$ = 2,18
Inc = 0,72
Azi = 220,3

σ_H = 1,56
σ_h = 1,49

Calculation of fracture:

$\sigma_x = 1{,}53$
$\sigma_y = 1{,}517$
$\sigma_{zz} = 2{,}18$
$\tau_{yz} = -0{,}0004$
$\tau_{xz} = -0{,}0082$
$\tau_{xy} = -0{,}0345$

$\theta = -39{,}67°$

$\sigma_r = Pw$
$\sigma_\theta = 2{,}91 - Pw$
$\sigma_z = 2{,}18$
$\tau_{\theta z} = -0{,}011$

$P_{wf} = 1{,}68sg$

Calculation of collapse:

$\theta = -34{,}68°$

$\sigma_r = Pw$
$\sigma_\theta = 2{,}91 - Pw$
$\sigma_z = 2{,}18$
$\tau_{\theta z} = -0{,}01$

$\sigma_1 = 2{,}915 - Pw$
$\sigma_1^{'} = 1{,}685 - Pw$

$$\sigma_3 = Pw$$
$$\sigma_3^{'} = Pw - 1{,}23$$

$$P_{wc} = 1{,}17\,sg$$

Appendix C

9/2-9S – 1867 mTVD

mTVD = 1867m
P_o = 1,03
$P_{w,sg}$ = 1,97
$O_{b,sg}$ = 2,04
Inc = 19,07
Azi = 282

σ_H = 1,64
σ_h = 1,58

Calculation of fracture:

$$\sigma_x = \left(1{,}64\cos^2 282 + 1{,}58\sin^2 282\right)\cos^2 19{,}07 + 2{,}04\sin^2 19{,}07$$
$$\sigma_x = \left(0{,}07089 + 1{,}5117\right)\cdot 0{,}893 + 0{,}2178$$
$$\sigma_x = 1{,}63$$

$$\sigma_y = \left(1{,}64\sin^2 282 + 1{,}58\cos^2 282\right)$$
$$\sigma_y = 1{,}569 + 0{,}0683$$
$$\sigma_y = 1{,}637$$

$$\sigma_{zz} = \left(1{,}64\cos^2 282 + 1{,}58\sin^2 282\right)\sin^2 19{,}07 + 2{,}04\cos^2 19{,}07$$
$$\sigma_{zz} = \left(0{,}07089 + 1{,}5117\right)\cdot 0{,}1067 + 1{,}822$$
$$\sigma_{zz} = 1{,}991$$

$$\tau_{yz} = \frac{1}{2}\left(1{,}58 - 1{,}64\right)\sin(2\cdot 282)\cdot \sin 19{,}07$$
$$\tau_{yz} = -0{,}03\cdot -0{,}4067\cdot 0{,}3267$$
$$\tau_{yz} = 0{,}00399$$

$$\tau_{xz} = \frac{1}{2}(1{,}64\cos^2 282 + 1{,}58\sin^2 282 - 2{,}04)\cdot \sin(2\cdot 19{,}07)$$
$$\tau_{xz} = \frac{1}{2}(0{,}07089 + 1{,}5117 - 2{,}04)\cdot 0{,}6175$$
$$\tau_{xz} = -0{,}14$$

$$\tau_{xy} = \frac{1}{2}(1{,}66 - 1{,}81)\sin(2\cdot 282)\cos 19{,}07$$
$$\tau_{xy} = -0{,}03\cdot -0{,}4067\cdot 0{,}94$$
$$\tau_{xy} = 0{,}011$$

Now the direction of the fracture has to be found:

$$\tan(2\theta) = \frac{2 \cdot 0{,}011}{(1{,}63 - 1{,}637)}$$
$$\theta = -36{,}54°$$

$$\sigma_r = Pw$$

$$\sigma_\theta = 1{,}63 + 1{,}637 - Pw - 2(1{,}63 - 1{,}637)\cos(2 \cdot -36{,}54) - 4 \cdot 0{,}011 \cdot \sin(2 \cdot -36{,}54)$$
$$\sigma_\theta = 1{,}63 + 1{,}637 - Pw + 0{,}0041 + 0{,}042$$
$$\sigma_\theta = 3{,}3131 - Pw$$

Uses axial stress, plane stress for simplicity:

$$\sigma_z = \sigma_{zz} = 1{,}991$$

$$\tau_{\theta z} = 2(0{,}00399 \cdot \cos(-36{,}54) - -0{,}14 \cdot \sin(-36{,}54))$$
$$\tau_{\theta z} = -0{,}159$$
$$\tau_{rz} = \tau_{r_\theta} = 0$$

$$P_{wf} = 1{,}63 + 1{,}637 - 2(1{,}63 - 1{,}637) \cdot \cos(2 \cdot -36{,}54) - 4 \cdot 0{,}011 \sin(2 \cdot -36{,}54) - \frac{-0{,}159^2}{1{,}991 - 1{,}03} - 1{,}03$$
$$P_{wf} = 2{,}26sg$$

Calculation of collapse:

Cohesion strength is equal to 0,2sg and angle of internal friction is equal to 30.

The direction where collapse will occur:

$$\tan(2\theta) = \frac{0{,}0115}{(1{,}63 - 1{,}637)}$$
$$\theta = -29{,}34°$$

$$\sigma_r = Pw$$

$$\sigma_\theta = 1{,}63 + 1{,}637 - Pw - 2(1{,}63 - 1{,}637)\cos(2 \cdot -29{,}34) - 4 \cdot 0{,}011 \cdot \sin(2 \cdot -29{,}34)$$
$$\sigma_\theta = 1{,}63 + 1{,}637 - Pw + 0{,}0073 + 0{,}038$$
$$\sigma_\theta = 3{,}3123 - Pw$$

$$\sigma_z = 1{,}991$$

$$\tau_{\theta z} = 2(0{,}00399\cos(-29{,}34) - -0{,}14\sin(-29{,}34)$$
$$\tau_{\theta z} = 2(0{,}00348 - 0{,}0686)$$
$$\tau_{\theta z} = -0{,}13$$

$$\sigma_1 = \frac{1}{2}(3{,}312 - Pw + 1{,}991) + \frac{1}{2}\sqrt{(3{,}312 - Pw - 1{,}991)^2 + 4 \cdot -0{,}13^2}$$
$$\sigma_1 = 2{,}625 - \frac{1}{2}Pw + \frac{1}{2}\sqrt{1{,}32^2 - Pw^2 + 0{,}0676}$$
$$\sigma_1 = 2{,}85 + 0{,}673 - \frac{1}{2}Pw - \frac{1}{2}Pw = 3{,}325 - Pw$$
$$\sigma_1^{'} = 3{,}325 - Pw - 1{,}03 = 2{,}295 - Pw$$
$$\sigma_3^{'} = Pw - 1{,}03$$

$$\frac{1}{2}(2{,}295 - Pw - Pw + 1{,}03)\cos 30 = 0{,}2 + \left[\frac{1}{2}(2{,}295 - Pw + Pw - 1{,}03) - \frac{1}{2}(2{,}295 - Pw - Pw + 1{,}03)\sin 30\right]\tan 30$$
$$\frac{1}{2}(3{,}312 - 2Pw)\cos 30 = 0{,}2 + \left[\frac{1}{2}1{,}265 - \frac{1}{2}(3{,}312 - 2Pw)\sin 30\right]\tan 30$$
$$P_{wc} = 1{,}17\,sg$$